Performance Analysis on Multi-Dimensional Optical Routing Networks

ZHANG Yu

A Thesis Submitted in Partial Fulfillment
of the Requirements for the Degree of
Master of Philosophy

in

Information Engineering

JULY, 2002

Acknowledgement

This thesis would have been impossible without the support of a host of people.

For most, I would like to express my warmest gratitude towards my research supervisor, Prof. Lian kuan Chen, for his guidance and support in my research and studies. I thank him for giving me valuable advice and enormous help. His working attitude and research ethics has been inspirational to me.

I would like to express my deepest appreciation to Prof. Calvin Chun-kit Chan. He was always there for questions and offer detail directions and helps.

Many thanks to Prof. Frank Tong, for his interests and comments with my research work and presentations.

Many members of the Lightwave Lab offer technical support and advice. I would particularly like to acknowledge Kit-Chan, Vincent Hung, Yong-gang Wen, Arthur Cheung, Jisong Wu, Jimmy Chan, Jorden Tswen, Scott Tam, Guo-wei Lu and Yi Yang. Your time and efforts are greatly appreciated.

Finally, thanks to my husband Yang Yang and my parents, for their continuous encourage, support and love.

Abstract

Deploying more than one optical multiplexing scheme in an optical network gives to the multi-dimensional network, which is promising for the explosion of traffic and growth of users on the Internet. In this thesis, the performance of a two dimensional code/wavelength routing network and the more generalized multi-dimensional optical routing networks have been studied and the results provide qualitative analysis on the benefits offered by the additional dimension or conversion capabilities.

The first part of the thesis presents the enabling technologies for three types of multi-dimensional optical routing networks, including the transmitters, optical switches/cross-connects and the optical conversion techniques. The blocking performance of a promising two-dimensional code/wavelength routing network is studied. The benefits of the deploying of code converters are shown by the code conversion gain.

The second part of the thesis investigated the performance of generalized multi-dimensional optical routing networks. Spatial decomposition and dimensional composition are proposed to facilitate the study. The blocking probability, link utilization and conversion gain of the network are derived with closed-form solutions by a generalized trunk switched model. The network topology is shown to have significant effects on these performances. Also, the utilization gain from additional dimensions is compared with the optical

conversion gain and the results can provide useful information on the network upgrading.

摘要

多維光網絡 (multi-dimensional network) 是指採用了多種光復用技術的混合光網絡，例如光時分/波分網絡（OTDM/WDM），光碼分/波分網絡(OCDM/WDM)等。它們通過增加頻道數目，減小帶寬粒度，來解決由於網絡中用戶增多和流量增大而造成的帶寬需求。本論文研究了多維光網絡的性質和性能，定性地分析了頻道轉換和新增維度帶來的增益，為現時網絡的升級提供重要的依據和信息。

論文第一部分介紹了實現三種重要的多維光網絡必需的技術和光器件，包括光源，光交換機和光頻道轉換技術 (optical conversion) 等。基於光碼分/波分網絡這種很有前途的 2 維網絡，文中研究其阻塞性能 (blocking performance)， 並且展示了引入碼字轉換器（code converter）所帶來的性能增益（code conversion gain）。

論文的第二部分研究了多維光網絡的性能和性質。文中提出了空間分解和維度分解兩種方法來簡化網絡阻塞性能的計算。計算了網絡的阻塞性能，鏈路利用率，和頻道轉換增益，並以顯式表達。結果顯示拓撲結構對多維網絡的各項性能均有重要的影響。 文中還比較了在波分復用網絡中引入新增維度（如時分復用技術）所帶來的增益和頻道轉換增益 (conversion gain)，所得結果能夠為網絡的升級提供有用的信息。

Contents

List of Figures

List of Tables

Chapter 1

Introduction

1.1 Overview of Optical Networking

In the last decade, optical networks have been deployed in modern communication networks to provide large bandwidth for the increasing demands of Internet users and voice users. *Optical Networking* is a hot field that attracts a lot of attentions. The concept of optical networking was first proposed in the middle 80's and the term has two main parts: the optical aspect and the networking aspect. It is defined as involving a network in which at least some of the operational steps in a network node take place in the optical realm, not just in the electrical realm. Two of the promising techniques in this field are *optical multiplexing* and *optical routing*.

Optical multiplexing is a kind of technique that can optically put multiple channels onto the backbone. It aims at enlarging the network capacity and providing bandwidth sharing among subscribers. Traffic explosion on the Internet makes the optical multiplexing extremely important in today's networks. The major undergoing optical multiplexing schemes are

- Optical Wavelength Division Multiplexing (WDM): WDM is the technology of combining a number of wavelength onto the same fiber. Conceptually, it is the same as frequency-division multiplexing (FDM) in microwave radio and satellite system. The key system features of WDM are the capacity upgrade, transparency, wavelength routing and wavelength switching.

- Optical Code Division Multiplexing (OCDM): In a network with optical

code division multiplexing, each channels is specified by a code. These codes are orthogonal to each other and can be used as symbols of the desired destination addresses. Therefore when tunable optical encoders and decoders are employed, one subscriber can communicate with any other user in the network. This gives to the optical code routing.

- Optical Time Division Multiplexing (OTDM): Time division multiplexing is a commonly used technique in electrical domain to achieve channel multiplexing. It is more complex and expensive to implement TDM in optical domain. There are two kind of OTDM network, namely *bit-interleaved OTDM* and *packet-interleaved OTDM*. In bit-interleaved networks, each channel occupies one time slot (bit) in a TDM frame. They have stringent synchronization requirement and the time slot (channel) tuning time should be of sub-nanosecond range when operate at high-speed. For packet interleaved TDM networks, the data packets from different nodes are transmitted in burst-mood and arrived asynchronously at the receivers.

- Subcarrier Multiplexing: Subcarrier multiplexing is a flexible technique for sharing the optical bandwidth among many subscribers. Single wavelength is used and each channel is represented by a specific RF subcarrier. The RF is mature and the RF components are economical and have good stability. However, the signal processing can only be done in electrical domain and the capacity is limited by various of noise such as thermal noise, shot noise, relative intensity noise, intermodulation products, clipping and optical beat interference.

- Polarization Division Multiplexing (PDM): By using different polarization states, TE and TM, to carry different optical data stream, polarization division multiplexing can double the bandwidth efficiency of a fiber. However, polarization control is needed to maintain the state of polarization.

Networks deploying one of these optical multiplexing schemes are generalized as *one-dimensional networks*. Hybrid networks deploying more than one type of optical multiplexing were also extensively investigated, which are

termed as *multi-dimensional networks*. They are dedicated to provide more channels and further increase the network capacity in order to adapt to the ever-growing traffic and network users.

Besides optical multiplexing, optical routing is another competitive and attractive technique for constructing all-optical networks. Generally, the current optical networks can either be opaque or all-optical, in another word, transparency. In opaque networks, optical-electrical-optical conversion or regeneration is performed at every intermediate node in the network and leads to the bottleneck of the network. All-optical networks, on the contrary, have no electrical signal regeneration or optical-electrical conversion. The communication between each node pair is carried out by an end-to-end optical *lightpath*, where the lightpath represents direct optical connection without any intermediate electronics. Each router (at the node) is able to read the addresses and other information carried in photon. This mechanism is called optical routing. Fibers, wavelengths, time slots, and even codes can be recognised by the optical layer, thus can represent the optical address of the desired destination and be used for optical routing. With optical routing, a network can support different bit rates, protocols and formats. Since there is no optical-electrical conversion at each node in the network, the total transmission at each node will be reduced and is a promising solution for the network bottleneck. Because of the long propagation delays, and the time required to configure the optical routers, optical routing networks are expected to operate in circuit-switched mode.

When optical routing is deployed in a one- or a multi-dimensional network, the network is termed as *one-dimensional optical routing network* and *multi-dimensional optical routing network*, respectively. Although as an extension of one-dimensional optical routing networks, multi-dimensional optical routing networks have unique properties in the aspects of device implementation, network management, control and the performance.

1.2 Mechanism in Optical Routing Networks

To illustrate the optical routing clearly, a wavelength routing network, which is most popular nowadays, is used as an example. As shown in Fig.1.1, it is a

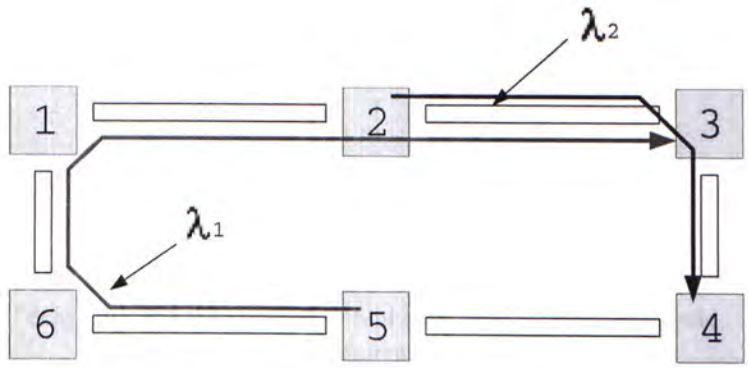

Figure 1.1: Wavelength routing in a ring network.

two-wavelength network with a ring topology. The optical signal between each node pair should be carried out on the same wavelength on all hops from the source to the destination. It is seen from Fig.1.1, the traffic from node 5 to node 3 is carried on λ_1, on all of the three hops of the lightpath. At the same time, node 4 is having a session with node 2 on wavelength channel λ_2. Under this scenario, the request for a session between the node 3 to node 6 is blocked. This kind of blocking can be released with the use of wavelength converters. The converter can translate the signals from an incoming wavelength channel to another wavelength channel optically. With a wavelength converter at node 5, lightpath from node 3 to node 6 can be established. The wavelength channels used on the successive three hops are λ_1 (from node 3 to node 4), λ_1 (from node 4 to node 5) and λ_2 (from node 5 to node 6). From above illustration, we can see that wavelength routing is able to overcome the scalability constrains through wavelength reuse, wavelength conversion and optical switching when the network extends to wide area. Therefore it is an important mechanism for optical transport networks.

1.3 Related Work on Optical Routing Networks

Related to the optical routing networks, there are many issues that are worth and desired for studying as shown in Fig.1.2. The first issue is the supporting or the enabling technologies, such as the optical converters and the optical

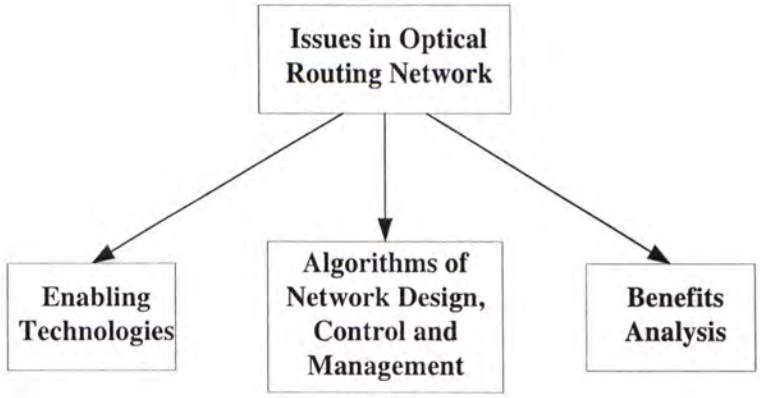

Figure 1.2: The issues with an optical routing network.

switches/cross-connects. The second is about the network design, control and management, such as the network protection and restoration. Another issue is the performance analysis on the network improvements, for instance, when optical converters or efficient routing and channel (wavelength) assignment algorithms are deployed in the network.

For the last aspects, hundreds of studies were reported in literature. Most were on the WDM networks with wavelength routing, since wavelength routing networks are more mature than other optical routing networks. Routing and wavelength assignment (RWA) algorithms, both static and the dynamic, were extensively studied [1, 2, 3, 4, 5]. The performance of wavelength routing networks with wavelength conversion have been widely studied through many different models [6, 7, 8, 9, 10]. In particular, optical networks based on sparse wavelength converters placement and limited conversion range have also been analyzed because of the high cost of the wavelength converter and its impairment to the transmission [11, 10]. We present below, in Table.1.1, a brief review of the fundamental models available. Binomial model, which is utilized in [6, 10] to describe the distribution of the number of busy channels on a link, has the lowest computational complexity among all the models and is used to indicate the qualitative behavior of the networks.

Authors	Kovacevic [7]	Subramaniam [11]	Birman [12]	Barry [6]
Traffic	Dynamic	Dynamic	Dynamic	Steady-state
Arrival Process	Poisson	Poisson	Poisson	Unspecified
Holding Time	Exponential	Exponential	Exponenetial	Unspecified
Routing	Fixed	Fixed	Fixed, Least-load	Fixed
Wavelength Assignment	Random	Random	Random	Random
Link Loads	Independent	Correlated (Markovian)	Dependent	Correlated Markovian
Wavelength on Adjacent Links	Independent	Dependent	Independent	Dependent
Performance Metric	Blocking Probability	Blocking Probability	Blocking Probability	Wavelength Utilization
Computational Complexity	Moderate	Moderate	High	Low

Table 1.1: Fundamental models for the performance analysis of wavelength routing networks

1.4 The Motivation of This Thesis

With the rapid growth of Internet users and service classes, future optical networks are desirable to offer high connectivity and large capacity. Wavelength routing networks, which employ wavelength division multiplexing (WDM), are the most promising solution for the near-term implementation of high capacity IP network infrastructure. In a wavelength routing network carrying circuit switched traffic, the whole bandwidth of a wavelength on each link is dedicated to a source-destination pair to carry the traffic between them. Although one wavelength can offer nearly the peak electrical transmission speed, without efficient bandwidth allocation, the low data-rate traffic will also take up the entire bandwidth of a wavelength and induce a very luxurious consumption of the resource. Moreover, limited number of wavelengths, which is around several tens per fiber nowadays, reduces the flexibility in bandwidth allocation and limits the bandwidth granularity for heterogeneous services in Internet traffic. Further improvement in performance, such as network utilization and blocking, can be achieved by several approaches. Firstly, wavelength conversion can be used to improve the flexibility of constructing an end-to-end lightpath, because it overcomes the constraint that the same wavelength should be employed on each hop of the lightpath [10, 11, 6]. Secondly, performance can be improved by adopting routing and wavelength assignment (RWA) schemes [13, 14, 15] at the expense of sophisticated control and management. Besides, by providing finer bandwidth granularity, more channels can be provided. Recent advances in Dense Wavelength Division Multiplexing(DWDM) enable the provision of more bandwidth as well as a larger number of channels. However, with the ever increase in the network size and the number of users, the limited number of available wavelengths, will be exhausted eventually. As an example, consider a 100-node network employing shortest-path-first-fit (SPFF) RWA scheme. If each node has 16 destination nodes, the number of wavelengths required is more than 200 [16]. By extending the channels to other dimensions such as time domain, frequency domain and code domain, the total number of available channels can be increased substantially. Thus, instead of using mere WDM technique, hybrid combination of WDM with OTDM, OCDM or SCM, the namely multi-dimensional networks, can offer large number of channels

and fine channel granularity [17, 18, 19, 16, 20]. Therefore, it is a promising solution for the explosion of traffic and subscriber on the Internet.

Blocking probability and network utilization are important indicators of network performance. In [16, 20, 19], the blocking performances of two-dimensional optical networks, as the multi-fiber multi-wavelength networks and TDM/WDM networks, were studied. However, the performance of generalized multi-dimensional optical routing networks is of more interest and needs to be investigated.

1.5 Thesis Structure

Because of the growing importance of the multi-dimensional optical routing networks and the lack of research work in this field, we presented the performance of generalized multi-dimensional optical routing networks, including the blocking probability, network utilization and optical conversion gain. Binomial model is used. The main contribution of the thesis is to extend the performance analysis from one-dimensional optical routing networks to the more generalized multi-dimensional optical routing networks. The results obtained can provide crucial information for the control and management of the multi-dimensional networks.

The thesis is arranged in the following:

Chapter1: Introduction
This chapter describes the two major aspects of optical networking: optical multiplexing and optical routing. Multi-dimensional optical routing networks are introduced. Previous work on the performance analysis of the wavelength routing networks are described. Also, the motivation of the thesis is presented.

Chapter2: Technologies for Multi-Dimensional Optical Routing Networks
This chapter introduces the technologies in supporting three types of multi-dimensional optical routing networks. Schematic and experimental setup of the transmitters, optical switches/cross-connects and optical converters etc. are presented.

Chapter3: Performance of Code/Wavelength Routing Networks
In this chapter, blocking performance of a reconfigurable optical code/wavelength routing network is studied, by the binomial model and a trunk switched model. The network blocking performances under various conversion capabilities are investigated and the blocking probabilities are given in closed-form expressions. Numerical results are obtained to show the performance improvement from the optical code conversion in terms of code conversion gain.

Chapter4: Decomposition Schemes
This chapter proposes two decomposition algorithms to facilitate the performance analysis of the *inclusive converted networks*, which is a class of multi-dimensional networks.

Chapter5: Performance of Multi-Dimensional Optical Routing Networks
In this chapter, we analyze the performance of a generalized multi-dimensional optical routing network with homogeneous switches. The closed-form network utilization is derived and compared to that of one-dimensional optical routing networks. Based on this analytical model, the closed-form conversion gains are derived for both partially and fully convertible cases. Besides, utilization gain from the addition of new dimensions is compared with the converison gain for a wavelength routing network.

Chapter6: Conclusion
This chapter concludes the thesis and points out possible future works.

Chapter 2

Technologies for Multi-dimensional Optical Routing Networks

2.1 Background

Exploring optical multiplexings and optical routing in the network are the key steps for constructing real optical networks, eliminating the bottle bottleneck of the electrical processing. To make this possible, newly developed optical devices and new optical techniques are desirable. Special transmitters, multiplexers/demultiplexers, optical fibers, and add/drops are necessary for the optical multiplexings in a network. For the purpose of optical routing, optical switches/cross-connects are indispensable elements. Many big companies and famous institutes around the world, such as Corning, Lucent, NTT, NEC thrust into this field.

Before the investigation on the performance of multi-dimensional optical routing networks in the following chapters, it is essential to introduce the main enabling technologies in supporting the optical multiplexings and optical routing. In the following sections of this chapter, the main technologies for constructing three types of multi-dimensional networks are introduced.

2.2 Multi-fiber WDM Networks

With the advance in wavelength-division multiplexing (WDM) technology, optical networks with WDM are the most popular infrastructure for the IP network. A WDM network deploying wavelength routing is one of the most frequently studied subjects in optical networks. The multi-fiber wavelength routing network is the most popular 2-dimensional optical routing network. The architecture of this network consists of wavelength routers interconnected by fiber links. In supporting multi-fiber wavelength routing networks, the following devices and technologies are indispensable:

2.2.1 Phased-Array-Based WDM Device

A highly versatile WDM device is based on using an arrayed waveguide grating (AWG) [21]. It can function as a multiplexer, a demultiplexer, an add/drop element, or a wavelength router. It is one of the most successful devices for the mentioned functions, because it offers low loss, high port count and can be mass produced. The AWG is a generalization of 2×2 Mach-Zehnder interferometer multiplexer. One popular design consists of M_{in} input and M_{out} output slab waveguides and two identical focusing planar star couplers connected by N uncoupled waveguides with a propagation constant β. The lengths of adjacent waveguides in the central region differ by a constant value ΔL, so that they form a Mach-Zehnder-type grating, as shown in Fig.2.1. For a pure multiplexer, we can take $M_{in} = N$ and $M_{out} = 1$. The reverse holds for a demultiplexer, that is $M_{in} = 1$ and $M_{out} = N$. In the case of a wavelength router, we can have $M_{in} = M_{out} = N$.

2.2.2 Wavelength-tunable lasers

Many different laser designs have been proposed to generate spectrums of wavelengths needed for WDM. The basic options are: (1) an array of discrete DFB or DBR laser, (2) wavelength-tunable lasers, (3) a multiwavelength laser array. Among them, wavelength-tunable transmitter is the most favorite one. It is based on DFB or DBR structure, which has a waveguide-type grating filter in the lasing cavity. A tunable multi-section DBR laser is shown in Fig.2.2(a). Wavelength tunning is achieved by electrical current injection into

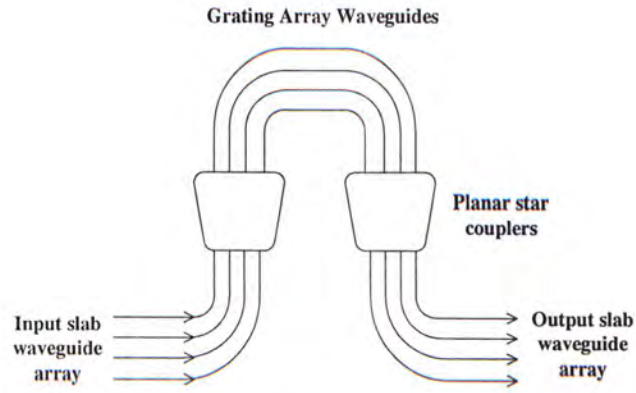

Figure 2.1: Top view of a typical arrayed waveguide grating used as a highly versatile passive WDM device.

the multi sections and the gain profile of the Coupler section shifts along the wavelength axis, as shown in Fig.2.2(b) [22]. Therefore, different wavelength can be selected as the output. This laser has a large tunning range of 40-60nm in the 1550nm window. It has a fast tunning speed of 5-100 ns and up to 100 channels are accessible.

2.2.3 Tunable optical Filter

A tunable optical filter is to select a desired channel from the backbone optically. Many technologies have been examined for creating them, such as the tunable MZI filters, tunable AWGs, and tunable multigrating filters. The schematic of a tunable multigrating filter used for add/drop is shown in Fig.2.3 [21]. The device operates as follows: a series of up to n wavelengths enter port 1 of the left-hand circulator and exit at port 2. In the untuned state, each fiber grating is transparent to all wavelengths. However, once a grating is tuned to a specified wavelength, this light will be reflected back, re-enter the left-hand circulator through port 2, and exit from port 3 to the demultiplexer. All the remaining wavelengths that are not reflected pass through to the right-hand circulator. They enter port 2 and exit from port 3. To add or reinsert wavelength that were dropped, one injects these to port 1 of the right-hand circulator. They first come out of port 2 and travel towards the series of tuned fiber gratings. The tuned gratings reflect each wavelength so that they head back towards the right-hand circulator and pass through it to combine with

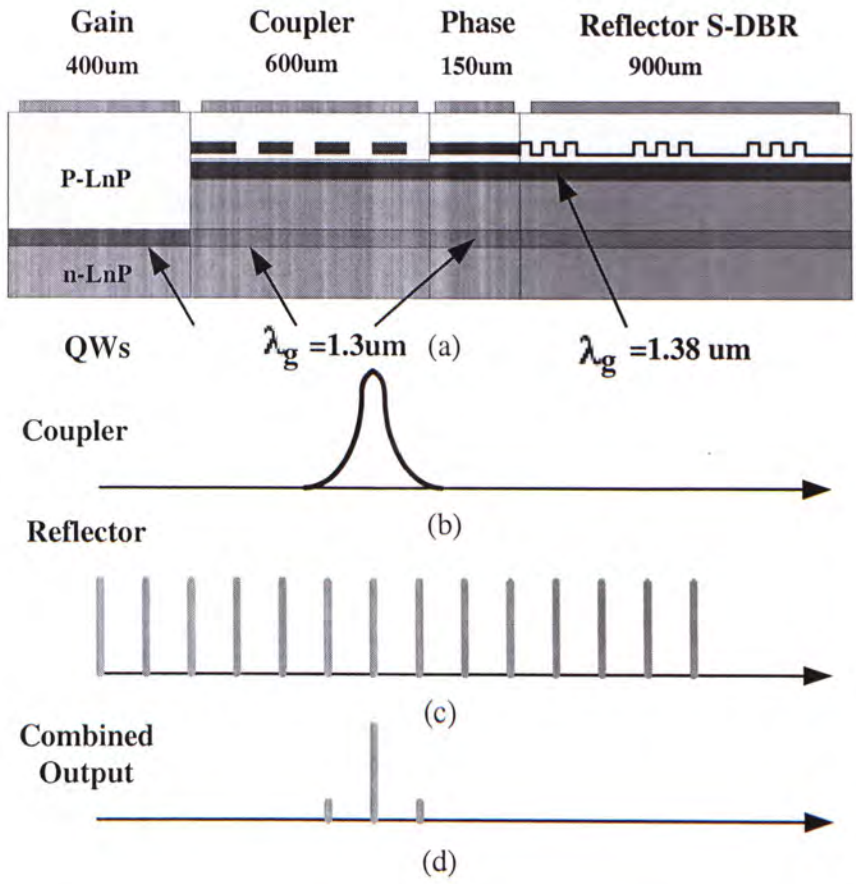

Figure 2.2: Schematic diagram of a three-section tunable distributed feedback (DFB) laser.

the other wavelength.

2.2.4 Wavelength Converter

Many approaches for wavelength switch were proposed [23, 24]. The schematic of the optical switch for the multi-fiber WDM network is shown in Fig.2.4. It is responsible for deliver the signal from one channel to any one of the output channels. In addition to the MUX, DMUX and the space switch, another desired element is the wavelength converter. As is stated, the wavelength converter is able to translate the wavelength optically. Therefore, it can improve the network performance by increasing the flexibility on the optical layer. The optical wavelength converter has been extensively studied during the last

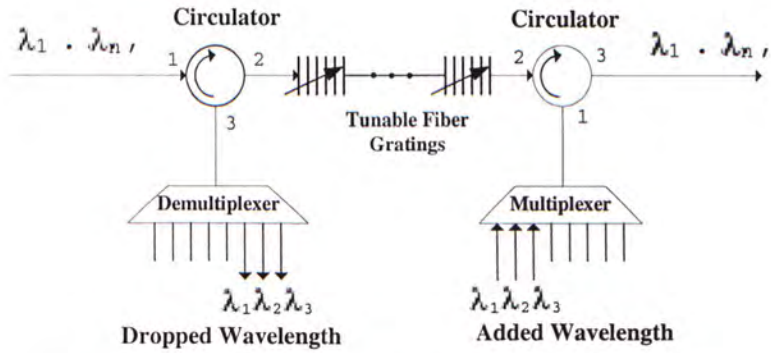

Figure 2.3: Multiple tunable filter grating used in conjunction with two optical circulators to add and drop any number of Ndifferent wavelengths.

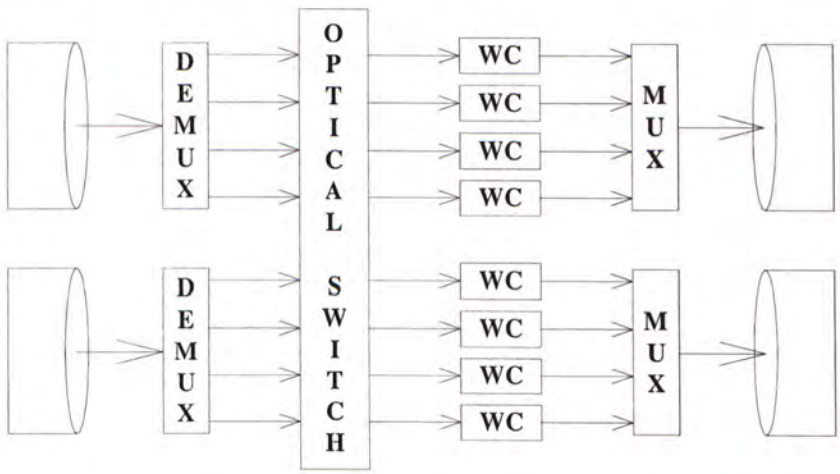

Figure 2.4: Schematic of the multi-fiber optical switch.

decade, both experimentally and theoretically [25, 26, 27, 28, 29, 30, 31]. The following are some techniques to achieve the function of wavelength conversion:

Four Wave Mixing (FWM)

Wave mixing arises from a nonlinear optical response of a medium when more than one wave is present. It results in the generation of another wave whose intensity is proportional to the product of the interacting wave intensities. Wave mixing preserves both phase and amplitude information, offering strict transparency. In Fig.2.5, $n = 3$ corresponds to four-wave mixing. The signal on λ_s and the pump on λ_p (continuous wave) are propagating simultaneously, and a third wavelength is generated on $f_c = 2f_p - f_s$ with the same pattern

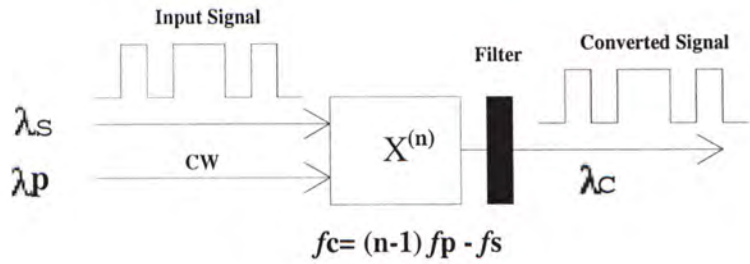

Figure 2.5: Schematic diagram of a wavelength converter based on FWM.

Figure 2.6: Schematic diagram of a wavelength converter based on XGM.

as the signal. This is the desired converted signal. This technique provides modulation-format independence and high bit-rate capabilities. However, the conversion efficiency is not very high and it decreases swiftly with increasing conversion span.

Cross Gain Modulation (XGM)

Semiconductor Optical Amplifier (SOA) could work in Cross Gain Modulation (XGM) and Cross Phase Modulation (XPM) modes. The principle of XGM is based on the gain saturation and on the homogeneous linewidth enhancement. Fig.2.6 shows a schematic diagram of the wavelength converter based on XGM. The intense signal pulse and the continuous probe wave co-propagate in the SOA. With bit "1" of the signal, the optical gain of the probe wave is small, while with bit "0", the probe wave has large optical gain. Therefore, the bit pattern of the signal is inversely converted to the probe wave's wavelength. An optical filter is used to remove the original signal.

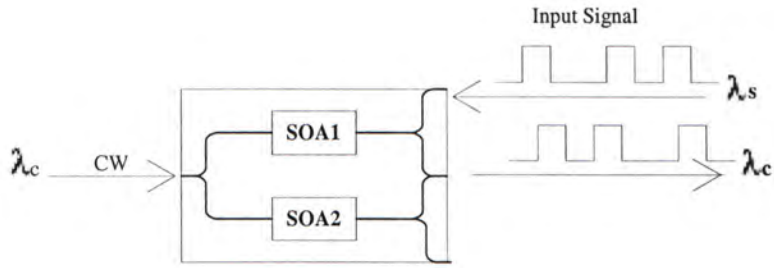

Figure 2.7: Schematic diagram of a wavelength converter based on XPM.

Cross Phase Modulation (XPM)

The operation of a wavelength converter using SOA in cross-phase modulation (XPM) mode is based on the fact that the refractive index of the SOA is dependent of the carrier level in its active region. An incoming signal that depletes the carrier density will modulate the refractive index and thereby result in phase modulation of a CW signal (λ_c) coupled into the converter. The SOA can be integrated into an interferometer so that an intensity-modulated signal format results at the output of the converter. Techniques involving SOA in XPM mode have been proposed using the nonlinear optical loop mirror (NOLM), Mach-Zender interferometer (MZI) and Michielson interferometer (MI). Fig.2.7 shows an MZI wavelength converter based on SOA in XPM mode. A continuous wave on λ_c is forward injected and splitted into the two arms with SOA. The signal power is injected backward. Phase of the CW lightwave on the upper arm changes with the bit pattern on λ_s. The constructive and destructive effect at the output coupler will make the light on λ_c having the same bit pattern with the signal.

With the XPM scheme, the converted output signal can be either inverted or non-inverted, unlike in the XGM scheme where the output is always inverted. The XPM scheme is also very power efficient compared to the XGM scheme.

2.3 OCDM/WDM

Recently, OCDM has been extensively investigated. Though it is not as mature and popular as its counter part in mobile communication, recent advances in

photonics devices, such as planar lightwave circuit (PLC) and super structure fiber Bragg grating (SS-FBG), have greatly enhance the feasibility of OCDM. In an OCDM/WDM network, which is a promising 2-dimensional network, bandwidth on one wavelength is divided into small fractions labelled by optical correlated codes, and assigned to different connections. Previous works include the experimental demonstrations of OCDM transmission systems as well as the code routing networks with optical code conversion [32, 33, 34, 35, 36, 37, 38]. More recently, the optical correlated codes are introduced as labels in a photonics multiple protocol label switching network (OMPLS), in order to simplify and speed up the processing in the Label Switched Router (LSR) [39, 40, 41]. The OCDM/WDM network would be a 3-dimensional network if multiple fibers are employed on each link. En/Decoding and optical code conversion are the desired optical technologies, which are listed below.

2.3.1 Optical En/Decoder

Several approaches are proposed for the optical en/decoding and two of them are described here.

Scheme1

An all optical 8-chip bipolar encoder is shown in Fig.2.8 [42]. It can generate all the possible combination of equi-amplitude 8-chip biphase shift keying (BPSK) codes by giving a binary phase shift of either 0 or π to the delay chip pulse on each arm. Note that the conventional n-stage ladder encoder can only produce limited number of codes. The delay time dt is set to 100ps, which is much smaller than the coherence time of the light source. The chip pulse width must be less than dt so that the chip pulse in a code is clearly resolved. The encoder can be used as the decoder by reversing the input and output ports. It is a monolithically integrated tapped delay line waveguide device fabricated on a silicate glass substrate by using Planar Lightwave Circuit (PLC) technology. The variable tap is a Mach-Zehnder interferometer waveguide. The thermal-optical phase shifter uses a Cr thin film heater. The code setup can be made by controlling the taps and the phase shifters using a desktop computer.

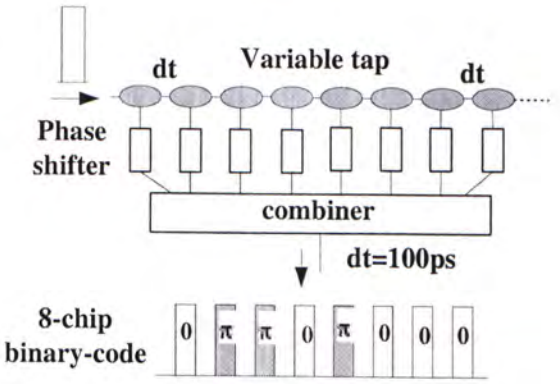

Figure 2.8: Experimental setup of optical code converter of scheme3.

Scheme2

Recently, optical en/decoder based on super-structured fiber Bragg grating (SSFBG) has been reported [43, 44, 45]. Fig.2.9 shows the schematic of a pulse encoding and decoding using SSFBG. The input pulse is reflected off SSFBG A, providing the transmission code which is a 7-chip pseudo random binary m-sequence. The length of each chip corresponds to the chip duration. After transmission, SSFBG B operates as a matched filter to despread the code sequence.

2.3.2 Optical Switch

A proposed CDM/WDM optical switch is shown in Fig.2.10 [40]. The composite signals on the different code/wavelength channels are first separated in the wavelength domain by an optical wavelength demultiplexer, and then decoded. The output from each decoder will feed into a time-gate-intensity-threshold (TGIT) device in order to differentiate the auto-correlation peaks from its sub-peaks and cross-correlation peaks, all generated from the decorrelated optical pulse train. At last, the decoded signal is switched to the desired output port of the space switch, recoded and transmitted again.

2.3.3 Optical Code Conversion

Similar to the wavelength routing, optical code routing is proposed and studied [38, 33]. Optical code conversion is an important issue for the optical code

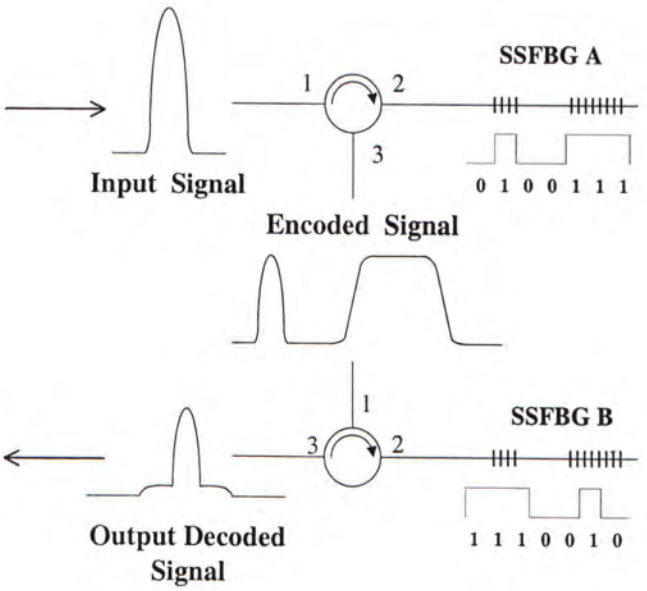

Figure 2.9: Outline of the physical approach of pulse encoding and decoding using superstructured fiber Bragg gratings (SSFBGs).

routing networks. It can be employed to improve the flexibility of the optical layer and make the optical code routing more efficient. Some experimental setups were proposed and two of them are listed here.

Scheme1

Fig. 2.11 shows a scheme for all optical code conversion [46]. The important distinction of this approach is the enabling code conversion that is independent of wavelength conversion and without alteration of other co-propagating codes. The schematic configuration is shown in Fig.2.11(a). It is a decode-and-recode approach. Fig.2.11(b) shows the experiment setup used to demonstrate code reconfiguration. A mode lock laser operating at 1557nm produced close to transform-limited laser pulse of width 2ps at a rate of 10 GHz. The significances of employing pulse train is the ability to gate in optical domain a decoded waveform to enhance the process gain of the scheme. These pulses were fed into a Lithium Niobate external modulator and on-off keyed at 10 Gbit/s using the data output of a pattern generator. The modulated pulse train was fed into a PLC encoder comprising eight equally spaced 5ps delays that employed a phase code sequence consisting of 0 or π. The encoded pulse

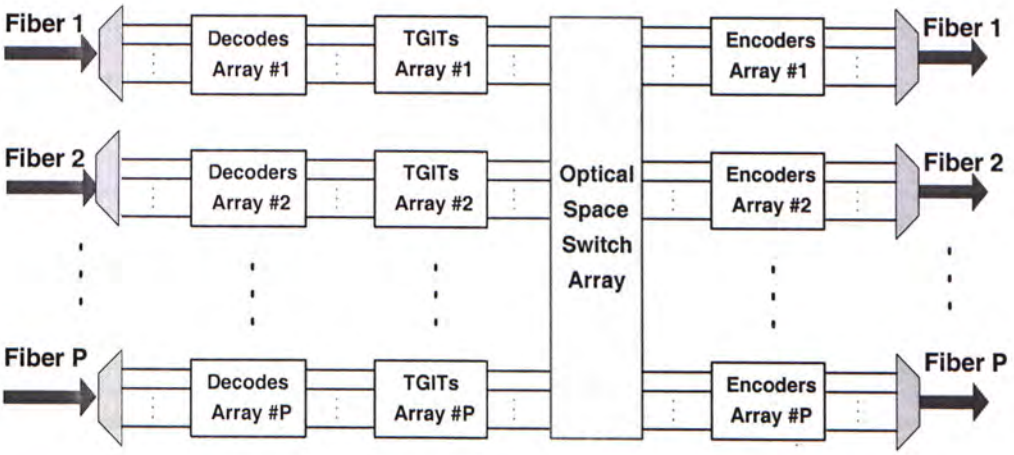

Figure 2.10: A proposed schematic of the OXC in a OCDM/WDM network.

train was fed into a PLC matched filter decoder. The output of the decoder was fed into a saturable absorber and combined with a high power 10-GHz pulse stream from a second mode locked laser driven from a RF source synchronized with the drive of first mode locked laser. The second mode locked laser, used to clock the gate at the autocorrelation peak, operates at a wavelength 1546.5nm, sufficiently offset to ensure that it may be removed by optical filtering when co-directionally pumped (this restriction on wavelength could be removed by pumping counter-directionally). The pump power at the input to the saturable absorber was 13dBm. The gate exhibits an extinction ratio of 15dB and a gate width 8ps. The gated pulse from the matched decoder was then fed to a second PLC encoder. Thus, the signal is optically translated from a code channel to another, where wavelength conversion is an independent process.

Scheme2

This scheme demonstrates an all-optical code conversion of 10Gb/s BPSK codes without wavelength-shift by using cross-phase modulation (XPM) in an optical filter [47]. The principle of the scheme is as follows. The index of the refraction corresponding to the signal light is modified through XPM proportionally to the instantaneous power envelope of the control light, resulting in a modulation of signal phase. In order to convert the optical BPSK code using XPM, the total phase shift during the interaction length must be π. And

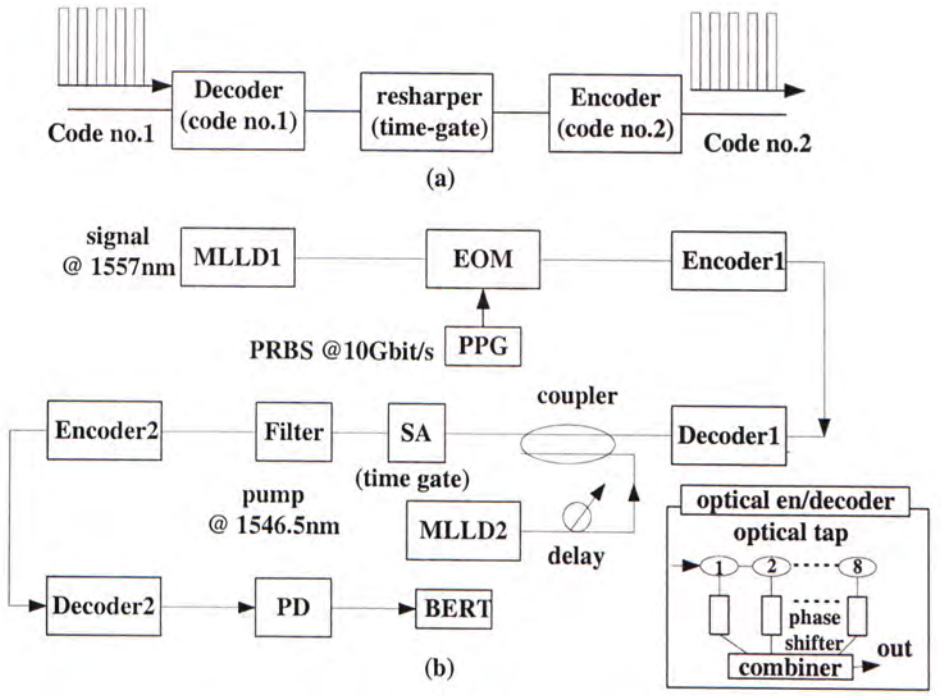

Figure 2.11: Experimental setup of optical code converter of scheme1.

in order not to shift the wavelength, the control pulse should walk through the entire signal pulse utilizing the group velocity dispersion (GVD). When the fundamental optical soliton is used as the control pulse, the difference of phase shift between the leading edge and tailing edge is minimized, because the shape of the control pulse is unchanged. Fig.2.12 shows the experiment setup. Transversal filter 1 is used as the optical encoder to generate time spread BPSK code. The signal BPSK pulse code sequences and the control pulse are combined together and launched into the DSF fiber. The optical code is converted by co-propagating with the control pulse in a DSF fiber through XPM. The output signal pulse sequence is matched filtered in the time domain by Transversal Filter 3. The output becomes the correlation waveform, which enables the verification of the code conversion.

2.4 OTDM/WDM

OTDM/WDM is another promising multi-dimensional networks because TDM is a commonly used mechanism for the bandwidth sharing. However, synchro-

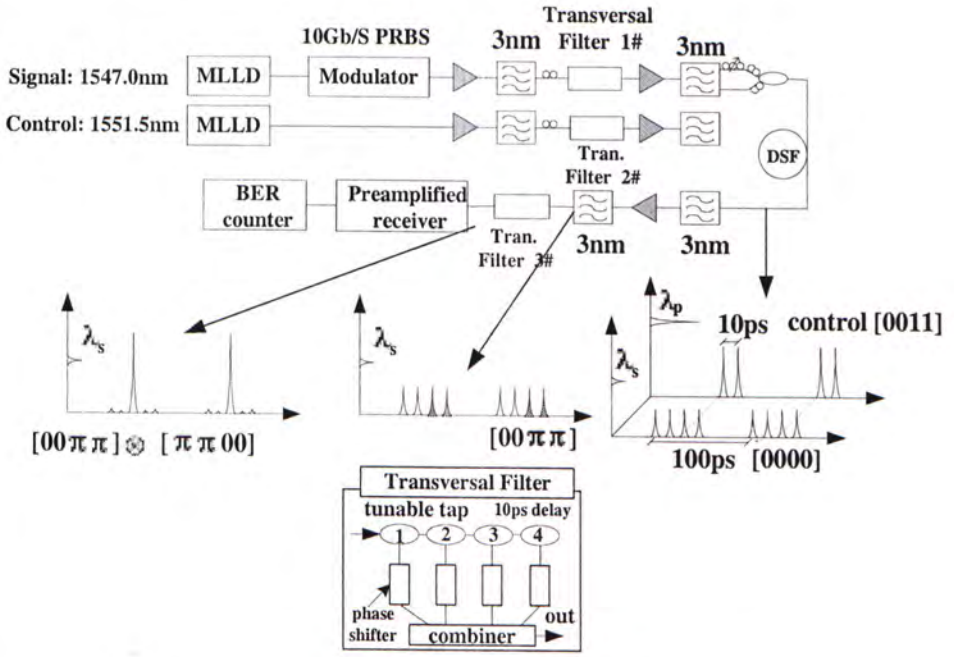

Figure 2.12: Experimental setup of optical code converter of scheme2.

nization among all the subscribers in the network is required.

2.4.1 Fast Optical Switch

In addition to lasers, MUX and DMUX which are needed as in a pure WDM network, another desirable device is fast switch with a wide operation spectrum. Many schemes are reported for constructing fast optical switches with new architectures and provide the possibility of the implementation of TDM/WDM network [48, 49, 50, 51]. Among all the approaches, semiconductor optical amplifiers (SOA) have been considered as promising candidates to fulfill this function because of their wide gain spectrum and possibility of being integrated with other optical devices.

2.4.2 Optical Time Slot Interchanger (OTSI)

Optical TSI is an optical converter which can interchange the signals in different time slots [51, 52, 53]. One of the schematic diagram of OTSI experimental system is shown in Fig.2.13. Its operation principle is described as follows. The DFB laser is directly modulated by a programmable pattern generator (Patt1)

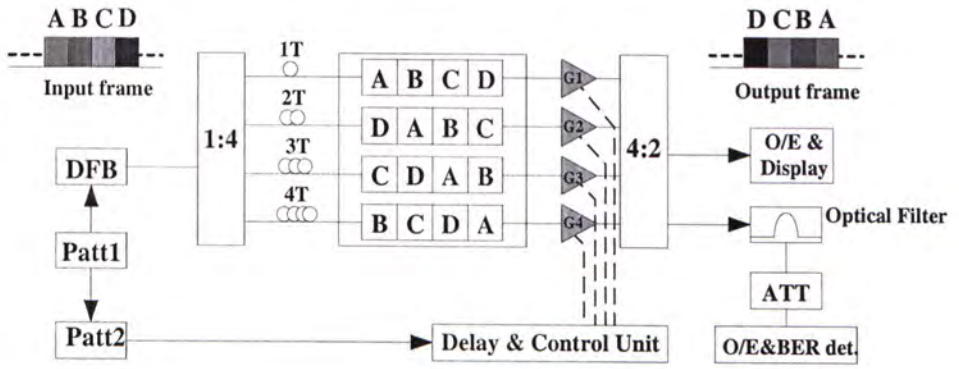

Figure 2.13: Schematic diagram of optical TSI experimental system.

at 2.5 Gbit/s. The input data frame consisted of four time slots or channels A, B, C, D, each containing a 16 bit data packet and a 4 bit guard band. This input signal to TSI is split into four parallel paths, each with different delay, before being fed into SLA (semiconductor laser amplifier) gates (G1-G4). A second pattern generator (Patt2), synchronized to Patt1, is used to produce a switch control pulse. The control pulse is fed into the delay and control unit to deliver the correct control signal to individual SLA gates according to assigned channel output. The gated signals are then recombined at a second passive coupler to form the new output. In this way, the signal in different time slots are interchanged.

2.5 Conclusion

In this chapter, three types of multi-dimensional optical routing networks, based on WDM, OTDM and OCDM, are demonstrated. The key devices and technologies for the implementation are introduced, including the transmitters, optical switches, optical filter and the optical converters. In addition to these networks, current technologies also offer the possibility for other hybrid networks, such as the SCM/PDM and TDM/CDM/WDM.

Chapter 3

Performance of Code/Wavelength Routing Networks

3.1 Background

Wavelength Division Multiplexing (WDM) network is a promising solution to the explosively growing bandwidth demand in today's internetworking. In addition to WDM, OCDM is another attractive optical multiplexing technology. It can further enhance bandwidth granularity of the WDM transport network and gives rise to the OCDM/WDM hybrid network. It is shown that, the spectrum efficiency of the OCDM/WDM network could be twice as much of that with WDM only [33]. Different from the wavelength routing in a conventional WDM network, in an OCDM/WDM network, an optical channel which is specified by an Optical Correlated Code (OCC) and a wavelength is assigned to a source-destination pair to carry the traffic between them. This is called *code/wavelength routing*. The enabling technologies are introduced in Chapter2. In this chapter, the main work focus on the blocking performance analysis of a code/wavelength routing network. Closed-form expressions are derived to show the improvement from the reconfiguration capability on the code dimension.

3.2 Reconfiguration Capability

For an optical network, one of the latest research thrusts is to enhance the optical layer control by increasing the reconfiguration capability of the network elements. In a simple wavelength routing network, wavelength converter is one of the most important reconfigurable elements. In an OCDM/WDM network, to enhance the reconfiguration capability of the optical layer, wavelength conversion (WC) and optical code conversion (CC) can both be utilized. Optical code conversion is used to translate input signals from one code channel to another code channel. Possible configurations are proposed recently in [33, 54], which have been described in Chapter 2.

Consider a OCDM/WDM network with single fiber for each link. Let H denotes the number of hops along a path, N denotes the number of wavelengths per fiber and M represents for the number of code channels per wavelength. Therefore all together $M \times N$ channels exist on a link. Every code/wavelength channel could be uniquely represented by a set of (h, n, m) , representing its indices of the hop, the wavelength and the code, respectively, where $1 \leq h \leq H$, $1 \leq n \leq N$, $1 \leq m \leq M$. The four types of routing nodes in a code/wavelength routing network can be described by their transfer functions T as below:

- The non-convertible routing node (NR)

  The node is only used for interconnecting fiber links and does not have any optical conversion capability. The input optical signal can only be put on the same code/wavelength channel on the output fiber. As it is shown in Fig.3.1(a), the input channel is (h, n, m), and the possible channel of the output link is represent by the hatched square in the link of $h + 1$. The transfer function of such a node can be described as $T_N(h, n, m) = (h + 1, n, m)$.

- The code convertible routing node (CR)

  This node could implement code conversion for the code channels, keeping the wavelength of the input signal unchanged. Shown in Fig.3.1(b), the input signal on (h, n, m) can be converted to any code channel on the

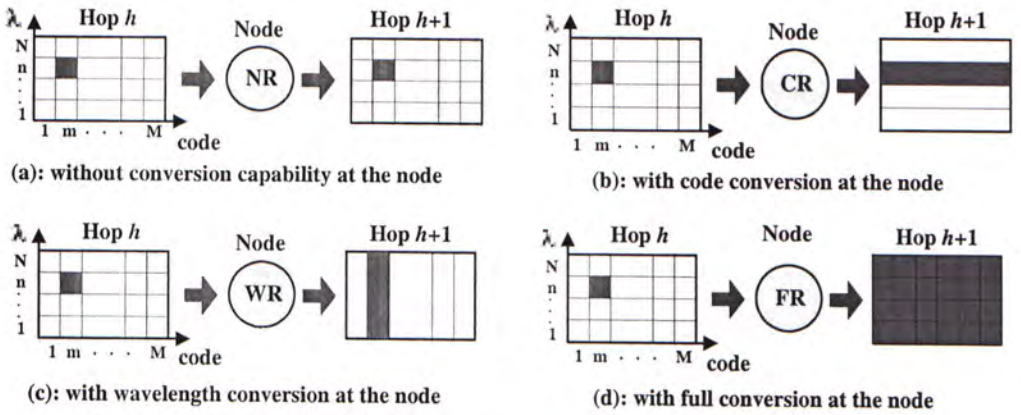

Figure 3.1: Possible channels for conversion to establish connections on the adjacent hops in a code/wavelength routing network.

wavelength n. The transfer function can be represented as $T_C(h, n, m) = (h + 1, n, m')$, where $1 \leq m' \leq M$.

- The wavelength convertible routing node (WR)

  This node can implement wavelength conversion as shown in Fig.3.1(c). The input signal on (h, n, m) can appear at any wavelength channel on the code m. And the transfer function is $T_W(h, n, m) = (h + 1, n', m)$, where $1 \leq n' \leq N$.

- The full-conversion routing node (FR)

  The node has integrated functions of a wavelength and code conversion, which can route the input signal to any code/wavelength channel on the output port. As shown in Fig.3.1(d), its transfer function is $T_F(h, n, m) = (h + 1, n', m')$, where $1 \leq n' \leq N$ and $1 \leq m' \leq M$.

These four kinds of routing nodes give rise to different reconfigure capability in the optical network, which will benefit the network in the aspects of rerouting, optical restoration and protection. Employing WC and CC in the network, a much flexible optical routing is achieved because it eliminates the constraint of routing on the fixed code/wavelength channel from the source to the destination.

3.3 Analytic Models

In this section, the blocking probabilities in an optical code/wavelength routing network carrying circuit switched traffic are discussed, by a trunk switched model.

3.3.1 Trunk Switched Model

To study the performance of the TDM/WDM networks, trunk switched networks were first introduced in [20]. In a trunk switched network, channels on each link are grouped into several trunks according to the conversion capability of a node. For each trunk, it should employ a full-channel interchanger (FI) to interchange all the channels in the same trunk. The number of channels in a trunk is called *trunk size.*

A *tunnel* is defined as a sequence of identical channel bunch from the source to the destination. The end-to-end channel selection for establishing a lightpath should be kept in the same tunnel and cannot cross different tunnels. The tunnel is said *successful* when the end-to-end connections can be set up within it, or it is regarded as *blocked.*

Fig. 3.2 shows the node construction in a trunk switched network. Due to the different conversion capabilities at the nodes, the definition of a trunk may be different among different nodes. Here, the partial conversion capabilities on code or wavelength dimension are not modeled. Therefore, in a single fiber code/wavelength routing network, trunks at different nodes, which are shown in Fig.3.3, are described as below. To make it clear, in Fig.3.3, we present at each node an example of trunk by marking all the channels inside with red color and bold line.

- NR: With neither code nor wavelength conversion at the node, the link is viewed as $M \times N$ trunks with one channels per trunk by NR.
- CR: With only code conversion at the node, the channels on the same wavelength are group into one trunk and the link is regarded as N trunk with the same trunk size of M.
- WR: The node has wavelength conversion only, therefore the channels

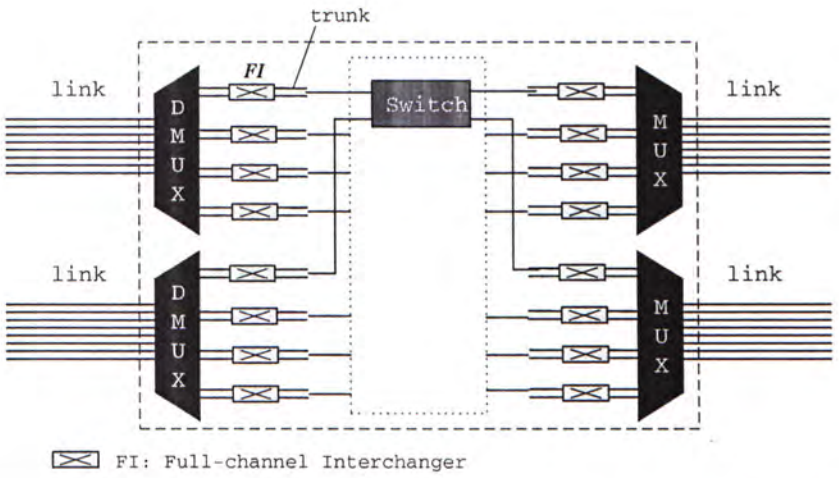

Figure 3.2: The architecture of a node in the trunk switched network.

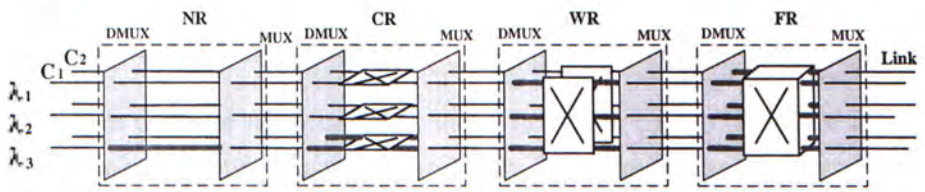

Figure 3.3: The trunks viewed by different nodes in a code/wavelength routing network.

on the same code channel are grouped into one trunk. The link therefore is regarded as M trunks and each has the same trunk size of N.

- FR: The node has both code and wavelength conversion, and the link is regarded as one trunk with the trunk size of $M \times N$.

3.3.2 Assumptions

For the performance analysis of the code/wavelength routing networks, the following assumptions are made:

- Each session uses the entire bandwidth of a channel;
- Uniform link load on each hop;
- Each channel is assumed to have the same busy probability ρ;

- The occupancy status of the channels (busy or free) on each link is assumed to be independent and thus is binomial distributed. Thus, the trunk statuses (busy or free) are independent, the number of busy trunks on a link is also a binomial distribution;
- The network only supports point-to-point traffic, ie, there is no multicasting and broadcasting;
- Circuit switched traffic is considered;
- Connection requests are not queued, ie, if a connection is blocked, it is immediately discarded;
- Static routing of connections. Thus connections between a particular source-destination pair always use the same fixed path, but may use any available channels on that path;
- Random channel assignment is used, in which connections are assigned to a channel which is chosen randomly from among available.

These assumptions are applicable for all of the following chapters of this thesis.

3.3.3 Blocking of the Paths with Various Configurations

Shown in Fig.3.4, user A requests for a session with user B through an H-hop path with various configurations. In the following, the blocking probabilities of the calls through these possible paths are investigated. The load and channel assignment on different links are assumed to be independent.

Case1: Path with no optical conversions

We first consider the case that there is no optical conversion allowed on the path, as shown in Fig.3.4(a). In order to setup the lightpath, the end-to-end connections should employ the same code/wavelength channel. This is the principle of code/wavelength continuity. The session will be blocked if all the $M \times N$ code/wavelength continuous lightpaths are blocked. Each code/wavelength channel has a load of ρ, which indicates the busy probability of a channel and also denotes the link utilization of the network. In this case, the blocking probability denoted by P_{B0} is:

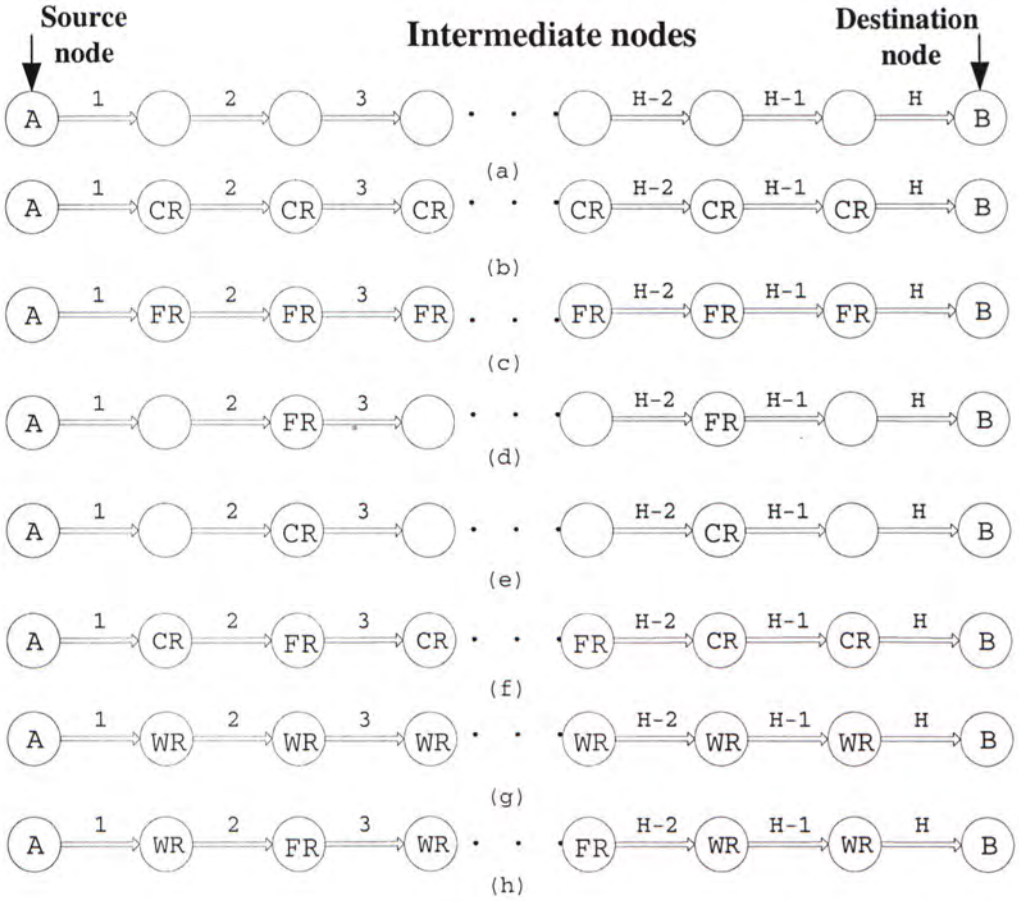

Figure 3.4: The paths with different reconfiguration capabilities.

$$P_{B0}(H, N, M) = \left(1 - (1-\rho)^H\right)^{NM}. \tag{3.1}$$

Case2: Path with CRs only

For a network deployed with code converters only, wavelength conversion still cannot be performed. Therefore, the wavelength continuity constrain should be obeyed during connections setup. A path with only code conversion is shown in Fig.3.4(b). According to the definition of the trunk, all the code channels on a wavelength on a link are regarded as a trunk, as illustrated in Fig.3.3. There are N trunks on each link, which equals to the number of wavelengths. When all the channels in a trunk are occupied, the trunk is

regarded as *busy*. Otherwise, the trunk is *free*.

Since each node has the same conversion capability in this case, the trunks viewed by each node are identical. So it is clear that, between the source and destination nodes, there are N fixed-wavelength tunnels which are considered independent. Because the N tunnels are identical, therefore, the blocking probability of an end-to-end path with H hops could be derived as:

$$P_{BC}(H, N, M) = \left(P\{a \textit{ fixed-wavelength tunnel is blocked}\}\right)^N .$$

Note that the blocking probability of each tunnel is equal to the blocking probability of the conventional wavelength routing network with wavelength converters as derived in [6]. A tunnel is successful when the trunk is free on each hop of this tunnel. Therefore, the blocking probability of a session when only CRs in the path can be expressed as:

$$P_{BC}(H, N, M) = \left(1 - \left(1 - \rho^M\right)^H\right)^N . \tag{3.2}$$

Thus we show that for this case, the original two-dimensional (code/wavelength) problem can be decomposed to one-dimensional problem. Similar results can be obtained for the case when there is WRs only.

Case3: Path with FRs only

For the case that all the nodes on the path are equipped with full-conversion, as shown in Fig.3.4(c), all the channels on a link are viewed as a trunk. Blocking would occur when any one of the H hops is blocked. In this case, we can consider the two-dimensional channels (N wavelength and M code) as one-dimensional channels with channel number $M \times N$. Thus the blocking probability can be derived as:

$$P_{BF}(H, N, M) = 1 - \left(1 - \rho^{NM}\right)^H . \tag{3.3}$$

Case4: Path with sparsely placed FRs only

The converter is expensive and therefore it is possible that only some nodes will be equipped with it. When full conversion is performed on some nodes

while other nodes have no conversion capability, as shown in Fig.3.4(d), the FRs will cut the path into K sub-path whose blocking probabilities are independent [10]. Within each sub-path, no conversion can be provided, which is equivalent to the case discussed in Case1. We assume a uniform placement of the converters. Under this scenario, according to the derivations above, the blocking probability can be expressed as:

$$P_{BSF}(H,N,M) = 1 - \prod_{k=1}^{K} P\{S^k = 1\} = 1 - \left(1 - \left(1 - (1-\rho)^L\right)^{NM}\right)^K, \tag{3.4}$$

where K is the number of sub-path. That means there are $(K-1)$ FRs are placed on the path. $P\{S^k = 1\}$ represents the success probability of the k^{th} sub-path. L is the average number of hops in a sub-path, where $L = \frac{H}{K}$. It must be noted that the expression in eq.(3.4) is exact only if H is an integer multiple of K, otherwise, the above equation is the lower bound of the actual blocking probability [10].

Case5: Path with sparsely placed CRs only

In this part we discuss the case that only code conversion is available and the code converters are sparsely placed as shown in Fig.3.4(e). We investigate the effect of code converters number on the blocking probability of the path. Because there is no wavelength conversion performed, the wavelength continuity constrain is required, thus at least one fixed-wavelength tunnel succeeds in order to set up an end-to-end connection. Similar to the discussion in Case2, there are N independent and wavelength-continuous tunnels. Each tunnel is further decomposed into K sub-path by the CRs. These subpaths are independent in blocking probability. The success probability of an end-to-end tunnel is:

$$P\{S_n = 1\} = \left(1 - \left(1 - (1-\rho)^L\right)^M\right)^K$$

For a call request, blocking occurs when all the N tunnels are blocked. In this way, the blocking probability of the path under the scenario of uniform

CRs placement is derived as:

$$P_{BSC}(H,N,M) = \prod_{n=1}^{N}(1 - P\{S_n = 1\}) = \left(1 - \left(1 - \left(1 - (1-\rho)^L\right)^M\right)^K\right)^N \tag{3.5}$$

Therefore, this problem is again simplified into a one-dimensional problem. Similarly, we can obtain the result for the path with sparsely placed WRs only.

Case6: Path with CRs and FRs

Another case that can lead to closed-form solutions is a path with CRs and FRs as shown in Fig.3.4(f). Assume that the FR nodes cut the path into K sub-segments which are independent as discussed above. Within each sub-path, there is no wavelength conversion permitted, and it is similar to the case discussed in Case2. The decomposition process of the path is illustrated in Fig.3.5. The blocking probability of the k^{th} sub-path, which is denoted by $P\{S^k = 0\}$, can be derived from equation eq.(3.3.3):

$$P\{S^k = 0\} = \left(1 - \left(1 - \rho^M\right)^L\right)^N$$

If the FRs are uniformly placed, the blocking probability of the path is derived as:

$$P_{BCF}(H,N,M) = 1 - \prod_{k=1}^{K}(1 - P\{S_k = 0\}) = 1 - \left(1 - \left(1 - \left(1 - \rho^M\right)^L\right)^N\right)^K \tag{3.6}$$

It is clear that in this case, a two-dimensional path is decomposed into one-dimensional paths to obtain the analytical results. Again we can obtain similar closed-form results for path with WRs and FRs.

In this section, the blocking performance in a code/wavelength routing network with different conversion capability has been investigated to obtain closed-form analytical results. We found that it is possible to obtain closed-form expressions of the end-to-end blocking probability in a two-dimensional routing path, by decomposing the two-dimension routing case into single-dimensional one. Fig.3.5 is an example showing the decomposition process

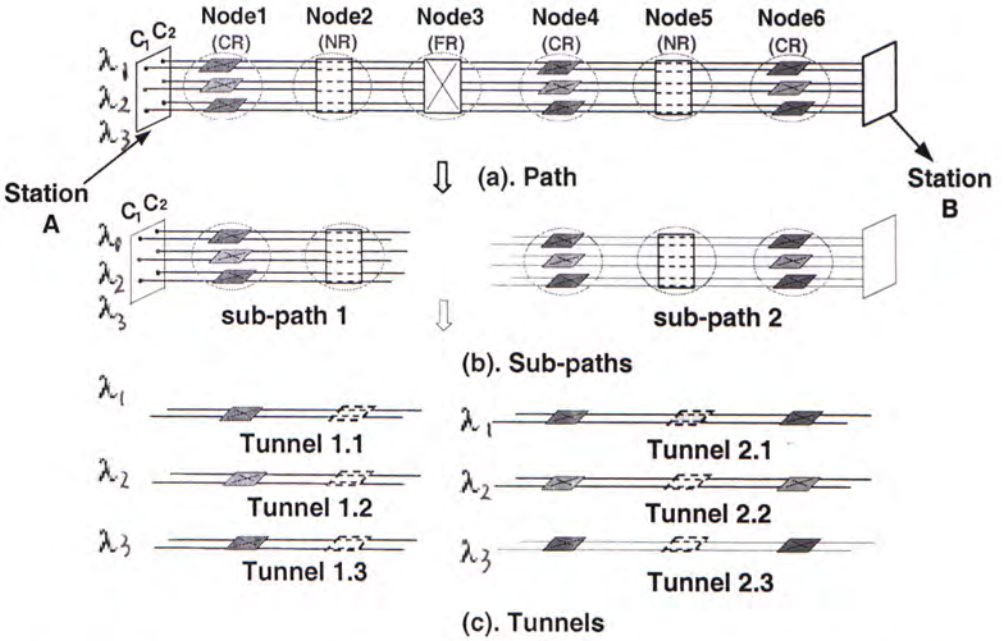

Figure 3.5: The decomposition procedure for the path with CRs, NRs, FR.

of the path with CRs, NRs, FRs. The decomposing principles can be extended to the generalized multi-dimensional optical routing path (the number of dimensions is larger than 1) to achieve closed-form expressions for end-to-end blocking probability. The generalization of the decomposition algorithm will be discussed in Chapter 4.

3.4 Numerical Results

From the derivations above, some numerical results are shown to illustrate the blocking probabilities and code conversion gains under various converter configurations. The improvement of the addition of conversion in the code dimension is demonstrated.

Fig.3.6 shows the blocking probability of a 20-hop path with different number of wavelengths and code channels. The total number of channels on a link is fixed at 16. From the graph, it is shown that the blocking probability is the highest when neither conversion is performed, no matter what the individual values of M and N are. With full conversion performed, the lowest blocking probability is achieved as expected. It is also found that with the aid of

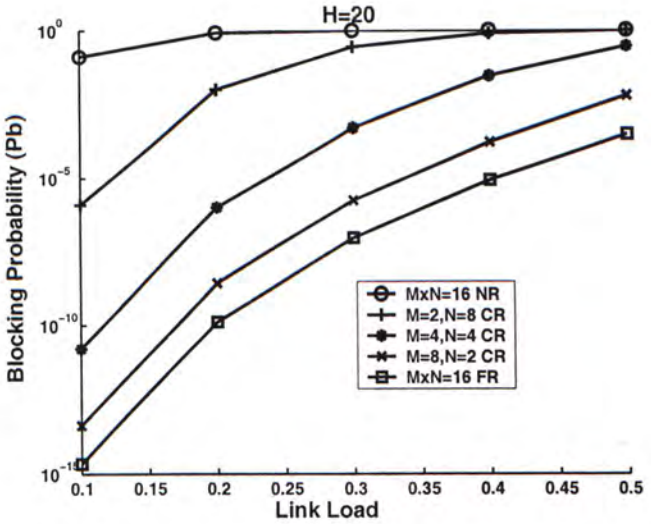

Figure 3.6: The Blocking Probability versus the link loads ρ.

code conversion, the blocking performance is improved significantly with the increase of the code number. Therefore, it is shown that when a large set of codes are employed, code conversion will bring significant improvement to the code/wavelength routing networks.

Code Conversion Gain is defined as the improvement in blocking probability when code conversion is added at the nodes on a path. Fig.3.7 shows the code conversion gain, which is the ratio of the blocking probability for the path of Case1 over that for Case5, when different number of code converters are placed. From Fig.3.7, we can find not only the code conversion gain increases with the increase of the number of code converter, but also the most significant improvement occurs at $\rho = 0.1$. Therefore, code conversion achieves higher conversion gain in a network with lower link load.

With code converters placed at some of the nodes, the path shown in Fig.3.4(g) becomes the path in Fig.3.4(h), since the combination of the code and wavelength conversion at a node gives rise to the FR. Here, the code conversion gain is the ratio of the blocking probability of the path in Fig.3.4(g)(with only WRs) to that of the path in Fig.3.4(h)(with WRs and FRs). The numerical result shown in Fig.3.8 demonstrates that, when code conversion uniformly added on four nodes of a 20-hop path, a significant gain of 10^4 is achieved.

Fig.3.9 shows the link utilization ρ of the paths in both Case5 and Case6

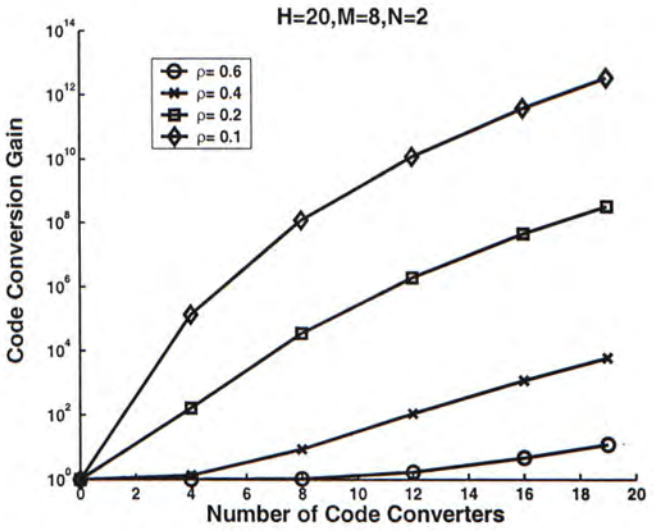

Figure 3.7: The code conversion gain versus the number of code converters along the path.

with $M = 8$, N= 8, $H = 20$. The required blocking probability P_b ($P_{BSC} = P_{BCF} = P_b$) are 10^{-3} and 10^{-5} respectively. We can see that when the allowed blocking probability increases from 10^{-5} to 10^{-3}, around 10% utilization improvement is achieved. In both case5 and Case6, the addition of code conversion will improve the link utilization, however the improvement is more significant in Case5. It is also found that, the link utilization increases most significantly when small number of the code converters are provided. For example, for the path in Case5, at a blocking probability of 10^{-5}, if only five nodes are provided with code conversion, the link utilization is increased by more than three folds. However even if all nodes are equipped with code conversion, the utilization gain is only around six folds.

3.5 Conclusion

In this chapter, the blocking performance and the link utilization of an optical code/wavelength routing network under limited conversion capabilities are investigated. By the mathematical analysis, closed-form expressions of the blocking probabilities are derived for various cases. The numerical results demonstrate the improvement from the code conversion in the network. For optical code/wavelength routing network with a small number of wavelengths

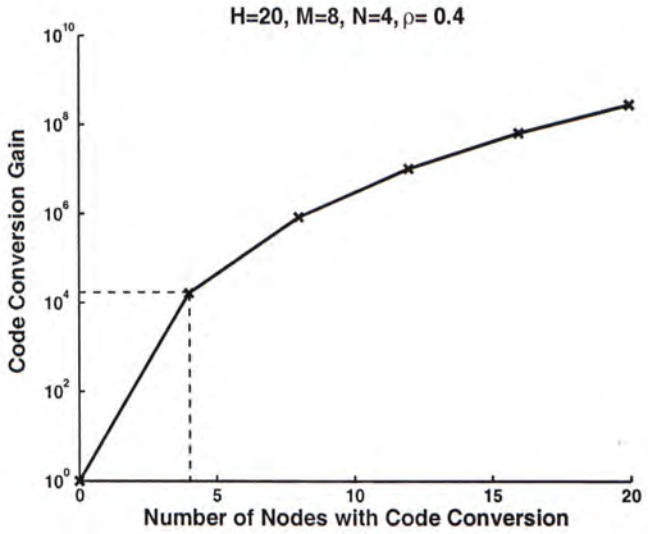

Figure 3.8: The code conversion gain when code conversion is sparsely added to the path already has WCs.

but a relatively large number of optical codes, code conversion will make significant performance improvements. For the low-loaded networks, code conversion will achieve high conversion gain. With wavelength conversion already provided in the network, the addition of the code conversion achieves a conversion gain as high as 10^4 even when the code conversion is provided with a low placement density (the ratio of the number of nodes with code conversion to the total number of nodes along the path) of 0.2. Thus, the code conversion could help achieve a higher throughput and an efficient utilization of the code/wavelength routing network.

Notation	Definition
WC	Wavelength conversion
CC	Code conversion
OCC	Optical correlated code
NR	Router without optical conversion
CR	Router with code conversion only
WR	Router with wavelength conversion only
FR	Router with both code and wavelength conversion
Trunk	A group of channels which can be fully interchanged at a node
Tunnel	A sequence of identical channel bunch from source to destination
M	Number of codes per wavelength
N	Number of wavelength per fiber
ρ	Uniform link load of the network
G	Conversion Gain (improvement on blocking probability)
H	Number of hops of a lightpath
K	Number of segments of a lightpath seperated by FRs
k	Index of segments
L	Number of hops per segment
n	Index of wavelengths
m	Index of codes
h	Index of hop number of a lightpath

Table 3.1: Notations used in Chapter 3.

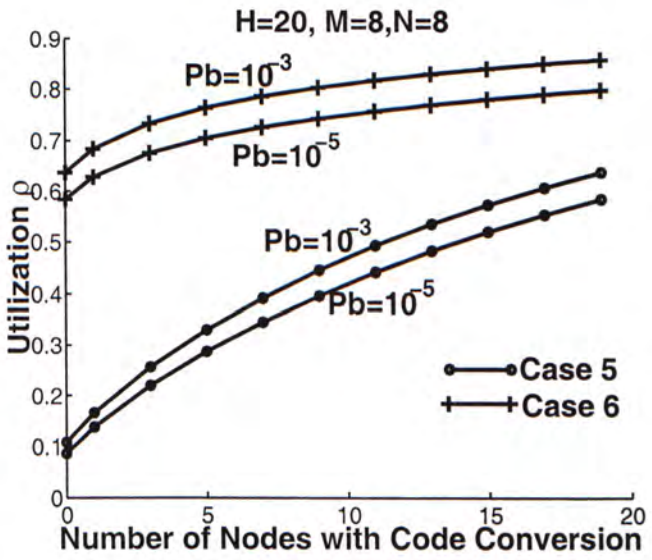

Figure 3.9: Link utilization versus number of nodes with code conversion. Pb: allowed blocking probability.

Chapter 4

Decomposition Schemes

4.1 Introduction

Hybrid optical networks, such as OTDM/WDM, OCDM/WDM and OTDM/CDM /WDM networks, bloom to offer higher transmission capacity and a larger number of channels [55, 37, 18]. With the recent advances in optical switching and optical devices, multiple optical switches have been reported to support multi-dimensional routing networks, e.g. time-space switches for the OTDM/WDM networks and space switches for the OCDM/WDM networks. In these hybrid networks, multi-dimensional optical multiplexing techniques are employed and individual channels can be switched independently at the node. On the other hand, optical conversion techniques, such as wavelength conversion, optical time slot interchanger, optical code conversion and multi-fiber space switches, are also widely investigated for providing reconfiguration capability on the optical layer, which have been introduced in Chapter 2. From this point of view, future optical networks would be heterogeneous switched networks. However, to the best of our knowledge, there was no paper investigating the blocking performance of multi-dimensional optical routing networks with heterogeneous switches. Motivated by the derivations on the blocking probability for the OCDM/WDM networks in Chapter3, in this chapter, we propose iterative decomposition schemes to facilitate the analysis of the quantitative behavior for a class of multi-dimensional routing networks.

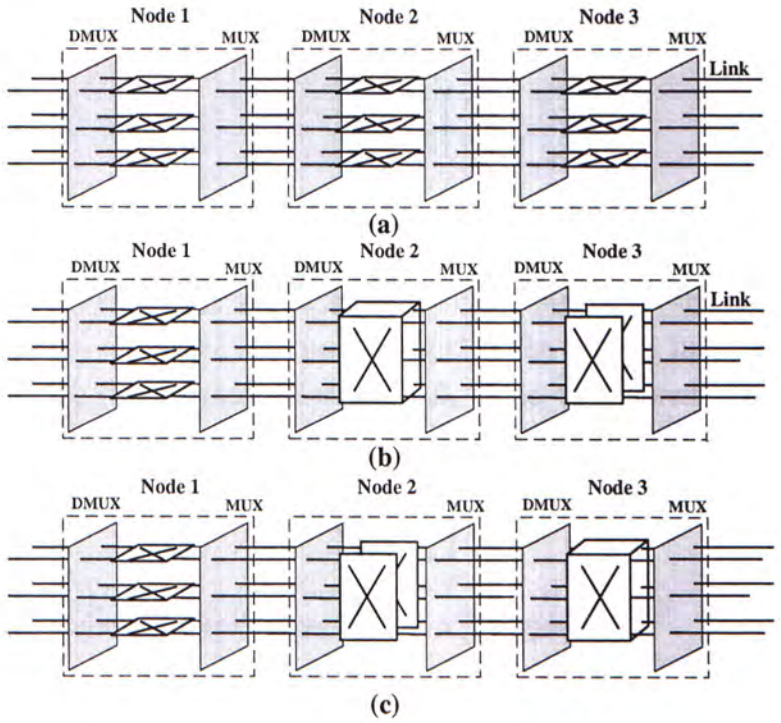

(a).Path in a homogeneous trunk switched network;
(b).Path in an inclusive converted trunk switched network;
(c).Paths in an exclusive converted trunk switched network.

Figure 4.1: Possible path configurations in a multi-dimensional trunk switched network.

4.2 Inclusive Converted Networks

Trunk switched model was described in Chapter3. In this chapter, we extend the trunk switched network to model generalized multi-dimensional networks (the number of dimensions is larger than 1).

As stated in Chapter3, in a trunk switched network, channels on each link are grouped into several trunks according to the conversion capability of a node. Each trunk employs a full-channel interchanger to interchange all the channels in the same trunk.

Assume a multi-dimensional network has a dimension set of D, where $D = \{d_1, d_2, ...d_i, ..., d_n\}$, n is the number of dimensions of optical multiplexing in the network. The number of channels on the dimension d_i is assumed to be

N_i and the total number of channels on a link is given by

$$N = \prod_{i=1}^{n} N_i \tag{4.1}$$

We generalize this network as an n-dimensional optical routing network ($n \geq 1$). Assume a node a in the network has the conversion capability on a set of dimensions E_a, where $E_a \subseteq D$. This means all the channels in the dimensions in E_a can be fully interchanged at the node a. In an n-dimensional network with heterogeneous switches, E_a could be different among different nodes. Therefore, for node a, the trunk size, which is denoted by M_a, is given by

$$M_a = \prod_{d_j \in E_a} N_j \tag{4.2}$$

And the number of trunks, denoted by K_a, is given as

$$K_a = \prod_{d_j \in (D - E_a)} N_j \tag{4.3}$$

Note that, $M_a \times K_a = N$.

In the general catalogue of the trunk switched networks, there are two classes of networks which are termed as *Inclusive Converted Networks* and *Exclusive Converted Networks*. For an inclusive converted network, the path inside should meet either of the following two conditions:

- $E_a \subseteq E_{a+1}$ and $E_a \subseteq E_{a-1}$,
- $E_a \supseteq E_{a+1}$ and $E_a \supseteq E_{a-1}$,

where, node a is any of the intermediate node on the path. When node a is the first intermediate node on the path, its neighbor on the left is the source node. Under this scenario, only E_{a+1} is considered. On the contrary, for the last intermediate node on the path, only E_{a-1} is considered. Other networks can be cataloged as Exclusive Conversion Networks.

Fig. 4.1 (b) shows an *Inclusive Conversion Path* in the inclusive converted network. In particular, when all the nodes has the same conversion capabilities, the network is a homogeneous network, which belongs to the general catalogue of the inclusive converted network. Fig. 4.1 (a) shows the path in

a homogeneous network. A path in the exclusive conversion network is shown in 4.1 (*c*).

Many multi-dimensional network can be modeled as an inclusive converted network, such as a multi-fiber code/wavelength routing network with optical code converters sparsely placed.

4.3 Decompositions

Two decomposition processes are proposed to study the performance of the multi-dimensional networks which can be modeled as inclusive converted networks. Binomial model is used and the loads on different links are assumed to be independent. Decompositions aim at partitioning the original path into sub-blocks that have fewer hops or dimensions and thus simplify the blocking probability calculation.

4.3.1 Spatial Decomposition (S.D.)

Spatial decomposition is adopted to separate the path into subpaths at the nodes with full conversion (FC) nodes. In a multi-dimensional network, the FC node refers to the node that has conversion capability on all the dimensional of the path and view all the channels in D as a trunk, such as the node 2 in Fig.(4.1) (b). The basic idea of S.D. lies in the assumption that, the blocking probability of the separated subpaths are independent [10]. Note that a path is divided into $k+1$ subpaths if it has k FC nodes. Under this scenario, the blocking probability of the path can be represented as:

$$P_B = 1 - \prod_{i=1}^{k+1} (1 - P_i) \tag{4.4}$$

P_i is the probability that a call is blocked at the i^{th} subpath. For each subpath, it can be regarded as a new path with the dimension set unchanged (D). Spatial decomposition is illustrated in Fig.3.5 in Chapter3. By S.D., the path in (a) is decomposed into two subpaths in (b).

4.3.2 Dimensional Decomposition (D.D.)

For a path that does not have FC nodes, *dimensional decomposition* is performed. The dimensional decomposition is based on the assumption that the channel on one link are independent.

Recall that, for a path with dimension set D, where $D = \{d_1, d_2, ...d_i, ..., d_n\}$, if none of the intermediate nodes has the conversion capability on a dimension d_i, then d_i is defined as *Non-Convertible Dimension.* On the other hand, for a dimension d_j in set D, if at least one node on the path can has conversion capability on it, d_j is termed *Convertible Dimension.*

Dimensional Decomposition begins at categorizing all the dimensions in D into convertible dimension set E and non-convertible dimension set $\bar{E}$, where $E + \bar{E} = D$. Let M be the total number of channels on the dimensions in set E. It is the product of the channel number of each dimension in set E, which is given by

$$M = \prod_{d_i \subseteq E} N_i \tag{4.5}$$

Similarly, the total number of channels K of set $\bar{E}$ is the product of the channel number of each dimension in the set $\bar{E}$, and

$$K = \prod_{d_i \subseteq \bar{E}} N_i \tag{4.6}$$

The path is viewed as K tunnels, with M channels in each tunnel. The tunnel, which has been defined in Chapter3, refers to as a sequence of the identical channel bunch from the source to the destination. Due to the conversion limitation at the nodes, the end-to-end channel selection should be kept in the same tunnel. These tunnels are independent in terms of blocking probability. Therefore the blocking probability of the path can be derived as:

$$P_B = \prod_{j=1}^{K} P\left(\textit{the } j^{th} \textit{ tunnel is busy}\right) = P_j^K \tag{4.7}$$

where P_j is the blocking probability of the j^{th} tunnel.

The dimensional decomposition is illustrated in Fig.3.5. By D.D., each subpath in (b) is decomposed into three tunnels.

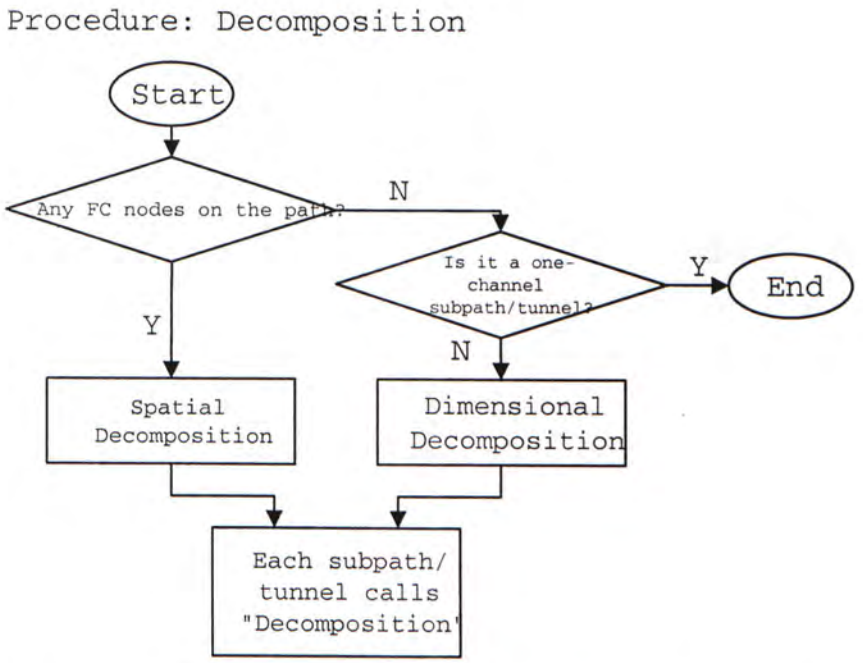

Figure 4.2: The flowchart of the iterative decomposition procedure for the inclusive converted network.

Due to the different conversion capabilities at the nodes, each tunnel can be regarded as a new path with heterogeneous switches and a dimension set E. In this way, by D.D., the path is decomposed into independent tunnels with a lower dimension of $|E|$. Notice that, each tunnel will also be an inclusive converted case.

4.3.3 Iterative Decompositions

An iterative decomposition scheme is proposed to analyze the qualitative behavior of an inclusive converted multi-dimensional routing network. The procedure is shown in Fig. 4.2.

For an inclusive converted path that has FC node, it is first operated by S.D., and is divided into subpaths. It should be noted that, because the original path is an inclusive converted path, then, at least one non-convertible dimension would exist in each subpath. Therefore, D.D. is operated on the subpath and decomposes it into independent tunnels. Although the tunnels on different subpaths may not be identical, new FC nodes will emerge in

each tunnel. Here, to a tunnel, the new FC nodes refer to the node that can permute on all the dimensions in it. As we know, each tunnel can be regarded as a new inclusive converted path. Then, again, we employ S.D. to divide the tunnel into subpaths at the new FC nodes, and so on. The decomposition is employed iteratively until only one-channel subpaths/tunnels with no conversion are obtained, and the decomposition procedure then stops. The blocking probability of the one-channel subpath/tunnel with hop number h, can be derived by

$$P_n = 1 - (1 - \rho)^h \tag{4.8}$$

where ρ is the busy probability of a channel and ρ is the number of hops of the one-channel subpath/tunnel.

According to eq.(4.4), eq.(4.7) and eq.(4.8), closed-form expression of the blocking probability of the original path can be obtained. If the original inclusive converted path has no FC nodes, the procedure will begin at D.D. first, and also stops when the one-channel subpaths/tunnels are obtained. A decomposition process for an inclusive converted path in a two-dimensional code/wavelength routing network is illustrated by the Fig.3.5 in Chapter3.

4.4 Conclusion

In this chapter, an iterative decomposition scheme is proposed to analyze the blocking probability for a class of multi-dimensional optical routing networks. Trunk switched model is extended to the generalized multi-dimensional case. This can lead to substantial simplification of the analysis and give quantitative assessment of the complex networks.

Notation	Definition
FC	Full conversion
D.D.	Dimensional decomposition
S.D.	Spatial decomposition
h	Number of hops of the one-channel subpath/tunnel
D	Dimension set of the optical multiplexings in a network
d_i, d_j	A dimension of the optical multiplexing of the network
E_a	The set of dimensions that node a has conversion capability on
k	Number of full conversion nodes on a path
E	Convertible dimension set
$\bar{E}$	Non-convertible dimension set
M	Total number of channels on the dimensions in set E
K	Total number of channels on the dimensions in set $\bar{E}$
N_i	Number of channels on dimension d_i
ρ	Link load, or the busy probability of a channel
M_a	trunk size viewed by node a
K_a	Number of trunk at node a
N	Total number of channels on the link

Table 4.1: Notations used in Chapter 4.

Chapter 5

Performance of Multi-Dimensional Optical Routing Networks

5.1 Homogeneous Trunk Switched Networks

Multi-dimensional homogeneous networks are a class of networks in which each node has the same conversion capabilities. In this chapter, we analyze their performance on the network utilization, utilization gain and optical conversion gain, by the extended homogeneous trunk switched model. Fig.4.1(a) shows a path in a homogeneous trunk switched network. The effect of the network topology on the network performance is considered.

In an n-dimensional homogeneous network ($n \geq 1$), the dimension set is denoted by D, where $D = \{d_1, d_2, ..., d_i, ...d_n\}$. The number of convertible dimensions is given by m, with $0 \leq m \leq n$, which means m out of the n dimensions are convertible. Thus the channels on these m dimensions can be fully interchanged on each node. For $m = 0$, it is a non-convertible network, for $0 < m < n$, it is a partial convertible network, and $m = n$ means a fully convertible network.

Each node has the same conversion capability in the homogeneous network, therefore the trunks viewed by each node are identical. Let K denote the number of trunks on each link and M denote the trunk size, or the number of channels per trunk. By the extended trunk switched model described in the section2 of Chapter4, they are given by

$$M = \prod_{i \in E} N_i, \; K = N/M = \prod_{i \in \bar{E}} N_i, \tag{5.1}$$

where E is the set of m convertible dimensions, and $\bar{E}$ is the set of $(n - m)$ non-convertible dimensions. N_i is the number of channels on the dimension d_i. N denotes the total number of channels on a link, which is given by eq.(4.1).

For a TDM/WDM network with L fibers per link, F wavelengths per fiber and T time slots per wavelength, it can be modeled as a homogeneous trunk switched network with $M = LT$ and $K = F$ if fiber switches and optical time slot interchangers are employed at each node.

5.2 Analytical Model

Based on the extended trunk switched network and the model for studying wavelength routing networks [6, 56], we proposed in this section an analytical model to evaluate the performance of the homogeneous multi-dimensional optical routing networks. Assume all channels have the same busy probability, or the channel utilization ρ. When all the channels in a trunk are occupied, the trunk is regarded as *busy*. Otherwise, the trunk is *free*.

In an optical routing network, the traffic originates from the source node may traverse more than one hop over the network and this leads to *link correlation* among the successive links. According to [20], link correlation ϕ is given by

$$\phi = \left(1 - \frac{1}{\bar{H}}\right) \frac{1}{\Delta}, \tag{5.2}$$

where $\bar{H}$ is the average number of hops of the lightpaths established in the network; Δ is the switch size, i.e. each node has Δ input links and Δ output links. Intuitively, the ring topology has a higher link correlation, compared to a hypercube network with the same number of nodes, because of the small switch size ($\Delta = 1$) and relatively large $\bar{H}$. Basically, link correlation ϕ represents the probability that a call is forwarded to the next hop along a path. Therefore, $(1-\phi)$ gives the probability that a call is dropped at one node. In this chapter, the correlation of the traffic on a link is assumed to be only due to its previous link, which is referred to as the *Markovian correlation*.

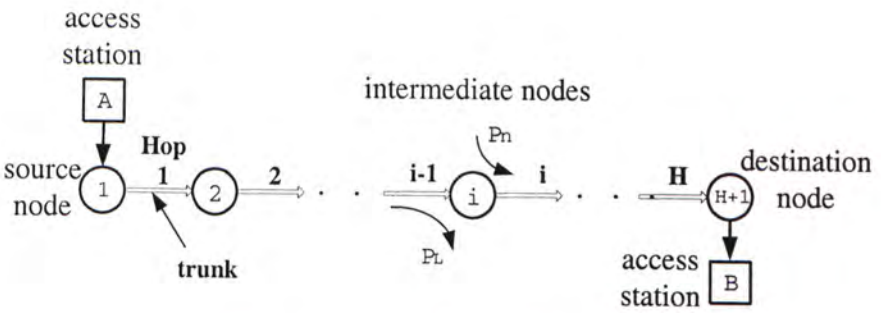

Figure 5.1: An H-hop call request.

As shown in Fig. 5.1, station A requests a session to station B over a mesh network. There are H hops (links) from the source node 1 to the destination node $H+1$. Due to the limited conversion capabilities at the nodes, channel selections on these H hops should be confined to the same trunk for establishing a lightpath. This is termed as *fixed-trunk constraint.* At node i, given that its input trunk is busy, let P_L be the conditional probability that at least one call is dropped from its input trunk, i.e. the trunk becomes free at node i. For a network with M channels per trunk, P_L can be derived as

$$P_L = \sum_{i=1}^{M} \binom{M}{i} (1-\phi)^i (\phi)^{M-i} = 1 - \phi^M. \tag{5.3}$$

Given that the input trunk of node i (the t_i in Fig.5.2) is free, P_n is the conditional probability that sufficient new calls are added at node i so as to make the output trunk (the t_o in Fig.5.2) become busy. That is

$$P_n = P\{\ t_o \textit{ at the node } i \textit{ is busy} \mid t_i \textit{ at the node } i \textit{ is free}\ \}. \tag{5.4}$$

There are three cases that will make the trunk on the i^{th} hop busy. The first case, as shown in Fig.5.2(a), is that all the channels in the trunk on the $(i-1)^{th}$ hop have calls, i.e. the trunk is busy, and all the calls are forwarded to the i^{th} hop. The second case is shown in Fig.5.2(b). The trunk on the $(i-1)^{th}$ hop is busy, with some of the calls leaving from node i, while new calls are inserted at node i to make the trunk on the i^{th} hop busy. As shown in Fig.5.2(c), the third case is that the trunk on the $(i-1)^{th}$ hop is free, i.e. there are free channels in this trunk, while new calls are inserted at the node i and make the trunk on the i^{th} hop busy.

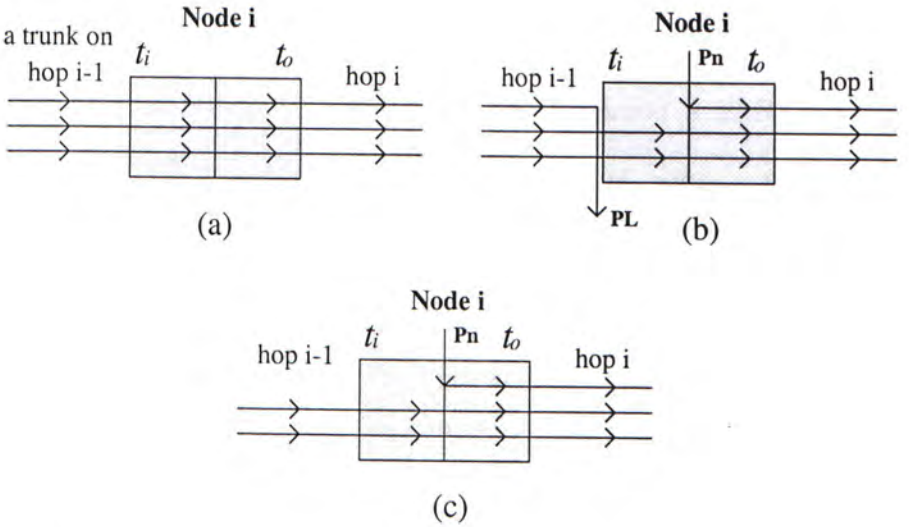

Figure 5.2: Three cases that make a trunk busy on the i^{th} hop. t_i and t_o are the input and output trunk of node i, respectively.

Extending the previous work in [6, 56] to the homogeneous trunk switched networks, the busy probability of the trunk on the i^{th} hop, denoted by q_i, can be derived as

$$\begin{aligned} q_i &= P\{\ t_o \textit{ at node } i \textit{ is busy}\ \} \\ &= P\{\ t_o \textit{ at node } i \textit{ is busy} \mid t_i \textit{ at node } i \textit{ is busy}\ \} P\{\ t_i \textit{ at node } i \textit{ is busy}\ \} \\ &+ P\{\ t_o \textit{ at node } i \textit{ is busy} \mid t_i \textit{ at node } i \textit{ is idle}\ \} P\{\ t_i \textit{ at node } i \textit{ is idle}\ \} \\ &= 1 \cdot q_{i-1}\,(1 - P_L) + P_n \cdot (1 - q_{i-1} + q_{i-1} P_L)\,. \end{aligned} \tag{5.5}$$

Therefore,

$$q_i = (1 - q_{i-1})\, P_n + q_{i-1}\,(1 - P_L + P_L P_n)\,. \tag{5.6}$$

In a network with K trunks per link and M channels per trunk, there are K end-to-end fixed-trunks, or tunnels, along the H hops. A lightpath can be established in any one of the tunnels, but not across different tunnels. Since all channels are assumed to be independent and have the same busy probability ρ, the busy probability of a trunk on the i^{th} hop is denoted by q_i and is simply

$$q_i = \rho^M, \quad 1 \le i \le H \tag{5.7}$$

Substituting (5.7) into (5.6), we obtain P_n as

$$P_n = \frac{\rho^M P_L}{1 - \rho^M + \rho^M P_L} \tag{5.8}$$

Further, assuming there is no blocking on both the ingress link (from station A to node 1) and the egress link (from node $H+1$ to station B), the blocking probability for an H-hop call requests (say from station A to B) is given by

$$\begin{aligned} P_b &= \prod_{k=1}^{K} \left(1 - \prod_{i=0}^{H-1} P_r \left\{ \begin{array}{c} \textit{the } k^{th} \textit{ trunk on} \\ \textit{the } (i+1)^{th} \textit{ hop is free} \end{array} \middle| \begin{array}{c} \textit{the } k^{th} \textit{ trunk on} \\ \textit{the } i^{th} \textit{ hop is free} \end{array} \right\} \right) \\ &= \left(1 - (1 - P_n)^H \right)^K . \end{aligned} \tag{5.9}$$

where 0^{th} hop ($i = 0$) represents the ingress link.

Combining (5.3)–(5.9) together, channel utilization ρ can be expressed by

$$\rho(M, K, H) = \left(\frac{1 - \left(1 - P_b^{\frac{1}{K}}\right)^{\frac{1}{H}}}{1 - \left(1 - P_b^{\frac{1}{K}}\right)^{\frac{1}{H}} \Phi(M)} \right)^{\frac{1}{M}} = \frac{\rho_0(M, K, H)}{\alpha(M, K, H)}, \tag{5.10}$$

where $\Phi(M) \triangleq 1 - P_L = \phi^M$ is defined as *trunk correlation* of the network. $\rho_0(M, K, H)$ and $\alpha(M, K, H)$ are given as follows,

$$\rho_0(M, K, H) = \left(1 - \left(1 - P_b^{\frac{1}{K}}\right)^{\frac{1}{H}} \right)^{\frac{1}{M}}, \tag{5.11}$$

$$\alpha(M, K, H) = \left(1 - \left(1 - P_b^{\frac{1}{K}}\right)^{\frac{1}{H}} \Phi(M) \right)^{\frac{1}{M}}. \tag{5.12}$$

Fig. 5.3 shows the relation between trunk correlation $\Phi(M)$ and trunk size M. Three types of networks are considered and their corresponding link correlations [20] are given beside the curves. As shown, trunk correlation $\Phi(M)$ decreases exponentially with respect to trunk size M.

$\rho_0(M, K, H)$ is the link utilization under the link independent assumption, i.e. link correlation $\phi = 0$. Note that, $\alpha(M, K, H) \leq 1$, therefore, under link independent assumption, the link utilization is underestimated, or, the blocking probability of the network is overestimated.

Further, as trunk size M becomes large, $\alpha(M, K, H)$ approaches 1 and $\rho(M, K, H)$, in turn, approaches $\rho_0(M, K, H)$. Therefore, the link independent assumption is valid only for the networks with large M values. This verifies the approximation applied in the calculation of link utilization for convertible wavelength routing networks[10, 6]. However, without wavelength

converters, the wavelength routing network is modeled as a trunk switched network with $M = 1$, and the effect of the traffic correlation is significant and cannot be ignored.

5.3 Utilization Gain

For an optical network with more than one dimension, it can provide finer bandwidth granularity by dividing the channel bandwidth of a one-dimensional network into fractions. Comparing a generalized n-dimensional optical routing network to a one-dimensional optical routing network with the same topology, the ratio of their link utilizations is defined as *utilization gain*, and is given as

$$G_u \triangleq \frac{\textit{Traffic carried in an n-dimensional network}}{\textit{Traffic carried in a one-dimensional network}}. \tag{5.13}$$

For both one- and n-dimensional networks without conversion capabilities, they can be modeled as trunk switched network with unit trunk size (i.e. $M = 1$). For the one-dimensional networks, the number of trunks per link, K, equals N_1, where N_1 is the number of channels per link. The link utilization for an H-hop path is denoted by $\rho\,(1, N_1, H)$, as derived from eq. (5.10). For an n-dimensional network, the number of trunks is $K = N$ and the link utilization of an H-hop path can be denoted by $\rho\,(1, N, H)$. Assuming the bandwidth on a link is fixed for both networks, the ratio of their link utilizations, or the utilization gain of an n-dimensional network is derived from eq.(5.10) and eq.(5.13) as:

$$G_u = \left(\frac{1 - \left(1 - P_b^{\frac{1}{N}}\right)^{\frac{1}{H}}}{1 - \left(1 - P_b^{\frac{1}{N_1}}\right)^{\frac{1}{H}}} \right) \left(\frac{1 - \left(1 - P_b^{\frac{1}{N_1}}\right)^{\frac{1}{H}} \phi}{1 - \left(1 - P_b^{\frac{1}{N}}\right)^{\frac{1}{H}} \phi} \right). \tag{5.14}$$

As $N > N_1$ and $\phi < 1$, the utilization gain G_u is greater than 1. Thereby, an optical routing network with finer bandwidth granularities gives a higher link utilization. As the total number of available channels, N, increases, the utilization gain will increase accordingly, but not linearly. When $N \gg 1$, $\rho\,(1, N, H)$ will be close to 1, and the utilization gain will approach $\frac{1}{\rho(1, N_1, H)}$.

Let $\phi = 0$, corresponding to the link independent case. The utilization gain is given by

$$G_u = \frac{\rho_0(1, N, H)}{\rho_0(1, N_1, H)} = \frac{1 - \left(1 - P_b^{\frac{1}{N}}\right)^{\frac{1}{H}}}{1 - \left(1 - P_b^{\frac{1}{N_1}}\right)^{\frac{1}{H}}}. \tag{5.15}$$

Comparing eq.(5.14) and eq. (5.15), it is found that the network utilization gain is scaled by a factor of $\frac{\alpha(1,N_1,H)}{\alpha(1,N,H)}$, which is less than 1, if the link correlation is taken into account. From the above illustration, it is found that the utilization gain is overestimated under the link independent assumption. The larger the N, the smaller the $\frac{\alpha(1,N_1,H)}{\alpha(1,N,H)}$, and the less accurate the link independent assumption is.

On the other hand, for a network with larger link correlation ϕ, $\frac{\alpha(1,N_1,H)}{\alpha(1,N,H)}$ falls and thus the utilization gain will decrease. Therefore, highly correlated network (with large value of ϕ) will obtain less significant improvement in link utilization when adding new dimensions.

Fig. 5.4 shows the utilization gain of a 3-dimensional optical routing network when the allowed blocking probability is $P_b = 0.001$. Different link correlation factors, ϕ, are considered. The numbers of channels on each dimension are N_1, N_2 and N_3, with $N_2 = N_3 = 16$, respectively. With the increase of N_1, the utilization gain decreases for all cases. $\phi = 0$ is the link independent case, which gives the maximum utilization gain. The utilization gain reduces with the increase of the link correlation ϕ.

Fig. 5.5 shows the utilization gain of the n-dimensional network ($n = 3$) versus the number of hops, H. Three networks with different link correlation ϕ are considered. It is shown that the utilization gain is fairly insensitive to the number of hops, H, when $H \geq 20$, disregarding the values of N_1 and ϕ. This result implies that the utilization gain of the n-dimensional network is fairly insensitive to the network size if the network is sufficiently large.

5.4 Conversion Gain

In this section, we apply the trunk switched model to investigate the performance improvement of a homogeneous n-dimensional network when optical

conversion is employed.

The networks before and after the additional conversions can both be modeled as homogeneous trunk switched network. To derive the conversion gain in the n-dimensional optical routing network, we model the original n-dimensional network as a trunk switched network with K_1 trunks and M_1 channels per trunk. After additional optical conversions are provided, the network can be modeled as a trunk switched network with K_2 trunks and M_2 channels per trunk.

For example, an optical routing network with F wavelengths and T time slots is regarded as a trunk switched network with $K_1 = FT$, $M_1 = 1$, when no conversion is provided. However, if only the optical time slot interchangers are provided, it will be modeled as a trunk switched network with $K_2 = F$, $M_2 = T$.

Notice that, $M_1K_1 = M_2K_2$ and $M_2 > M_1$. By substituting the parameters $\{M_1, K_1\}$ and $\{M_2, K_2\}$ to eq.(5.10), we can get the link utilizations before and after the optical conversion, denoted as ρ_1 and ρ_2, respectively. Hence, the utilization improvement $G_c = \frac{\rho_2}{\rho_1}$ is defined as the *conversion gain* and given by

$$G_c = \left(\frac{1 - \left(1 - P_b^{\frac{1}{K_2}}\right)^{\frac{1}{H}}}{1 - \left(1 - P_b^{\frac{1}{K_2}}\right)^{\frac{1}{H}} \Phi(M_2)} \right)^{\frac{1}{M_2}} \cdot \left(\frac{1 - \left(1 - P_b^{\frac{1}{K_1}}\right)^{\frac{1}{H}} \Phi(M_1)}{1 - \left(1 - P_b^{\frac{1}{K_1}}\right)^{\frac{1}{H}}} \right)^{\frac{1}{M_1}} \tag{5.16}$$

By making some appropriate simplifications and approximations (Appendix), the maximum value $G_{c,max}$ of the conversion gain is derived as

$$G_{c,max} < \left(H\left(1 - \phi^{M_1}\right)\right)^{\frac{1}{M_1} - \frac{1}{M_2}}, \quad M_2 > M_1 \tag{5.17}$$

It is found from the eq.(5.17) that the maximum utilization gain depends on the number of hops H, link correlation ϕ, the former trunk size M_1, and the trunk expanding factor ($S = \frac{M_2}{M_1}$). By keeping all the other parameters unchanged, the increase in S will lead to a higher conversion gain. However, with the increase in S, the maximum conversion gain will saturate quickly to

$$G_S = \left(H\left(1 - \phi^{M_1}\right)\right)^{\frac{1}{M_1}}. \tag{5.18}$$

Fig. 5.6 demonstrates the conversion gain when optical converters are added in an n-dimensional network that originally does not have any conversion. Three types of networks with different link correlations are investigated. N is the total channel number. The number of hops is $H = 20$. Three cases are considered. $M = N$ is the fully converted case while $M = \frac{N}{2}$ and $M = \frac{N}{4}$ are the partially converted cases. As illustrated in the figure, the network with a higher link correlation exhibits less significant conversion gain under the same scenario. For each type of network, maximum gain is obtained when the total number of channels N is about 10, 20 and 30 for $M = N$, $M = N/2$ and $M = N/4$, respectively. Also, the conversion gain is the highest when fully conversion is provided ($M = N$). However, even when the trunk size is as small as one quarter of the total channel N, the conversion gain is very close to the fully converted case, especially when N is large. This result implies, by providing optical conversion on the dimension even with small number of channels, the utilization improvement can be significant.

5.5 Comparison on the Utilization Gain by Multiplexing and by Conversion

For a wavelength routing network, it can be either upgraded to a convertible wavelength routing network by placing converters at the nodes or upgraded to a 2-dimensional networks by adding a new dimension, TDM, for example. From the derivations in the previous sections, these two approaches can both provide improvements in the link utilization. In this section, we will compare the improvements in the link utilization under these two approaches for a wavelength routing network.

Without the loss of generality, we assuming there are N_1 wavelengths on each link in the wavelength routing network and the number of channels in the additional dimension is N_2. After the addition of the second dimension in the wavelength routing network, by eq.(5.10) and eq.(5.13), the utilization gain is given as

$$G_{wu} = \frac{\rho(1, N_1 N_2, H)}{\rho(1, N_1, H)}. \tag{5.19}$$

When by applying wavelength converters into the network, from eq.(5.10)

and eq.(5.13), the conversion gain is derived as

$$G_{wc} = \frac{\rho(N_1, 1, H)}{\rho(1, N_1, H)}. \tag{5.20}$$

Fig.(5.7) shows the improvement in the link utilization of the network versus the number of hops H. The allowed blocking probability is $P_b = 10^{-3}$. N_1 and N_2 are assumed to be 8 and 16, respectively. It is found that, link correlation affects the conversion gain more significantly than the utilization gain by multiplexing (adding a new dimension). For a highly correlated network, as a ring with $\phi = 0.92$, the utilization gain by multiplexing is always larger than the conversion gain, no matter how large the network is. For the moderately ($\phi = 0.31$) and slightly (ϕ=0.09) correlated networks, when the network size is small, the addition of a new dimension can obtain a higher utilization gain than deploying converters.

Fig.(5.8) illustrates the improvement in the link utilization of the network versus the wavelength number N_1, with $N_2 = 16$ and $P_b = 10^{-3}$. For a highly correlated network, no matter how many number of wavelengths (N_1) it has, utilization gain by deploying a new dimension would be higher than the conversion gain. However, for the moderately and slightly correlated networks, only when the number of wavelength is small, the utilization improvement by multiplexing is more significant than the conversion gain.

5.6 Conclusion

In this chapter, an analytic model is proposed for studying the network utilization of generalized multi-dimensional optical routing networks. It is found that the utilization gain by multiplexing is closely related to the link correlation. Less link correlated network will achieve more significant utilization gain. It is also found that, the utilization gain is fairly insensitive to the network size. We derive, for the first time, closed-form solutions for the conversion gain in a partially or fully convertible n-dimensional optical routing network. From the comparison of the utilization gain by multiplexing with the conversion gain, we find that highly correlated networks can obtain higher utilization gain by multiplexing. Also, small networks and the networks with small number of channels also benefit more from multiplexing than from conversion.

Appendix

From eq. (5.11), we get:

$$\begin{aligned}\rho_{10} &= \left(1-\left(1-P_b^{\frac{1}{K_1}}\right)^{\frac{1}{H}}\right)^{\frac{1}{M_1}} \\ &\approx \left(-\frac{1}{H}ln\left(1-P_b^{\frac{1}{K_1}}\right)\right)^{\frac{1}{M_1}}.\end{aligned} \tag{5.21}$$

This approximation is valid for large H and $P_b^{\frac{1}{K_1}}$ not to close to one. For $P_b = 0.001$, $H = 10$, and K_1 is as large as 100, the error is within 5% and 0.5% for $M_1 = 1$ and $M_1 = 10$, respectively.

Similarly,

$$\begin{aligned}\rho_{20} &= \left(1-\left(1-P_b^{\frac{1}{K_2}}\right)^{\frac{1}{H}}\right)^{\frac{1}{M_2}} \\ &\approx \left(-\frac{1}{H}ln\left(1-P_b^{\frac{1}{K_2}}\right)\right)^{\frac{1}{M_2}}.\end{aligned} \tag{5.22}$$

And from eq. (5.12), we get:

$$\begin{aligned}\alpha_1 &= \left(1-\left(1-\rho_{1_0}^{M_1}\right)\Phi\left(M_1\right)\right)^{\frac{1}{M_1}} \\ &= \left(1-\Phi_1-\frac{1}{H}ln\left(1-P_b^{\frac{1}{K_1}}\right)\Phi_1\right)^{\frac{1}{M_1}},\end{aligned} \tag{5.23}$$

where $\Phi_1 = \Phi\left(M_1\right) = \phi^{M_1}$.

$$\begin{aligned}\alpha_2 &= \left(1-\left(1-\rho_{2_0}^{M_2}\right)\Phi\left(M_2\right)\right)^{\frac{1}{M_2}} \\ &= \left(1-\Phi_2-\frac{1}{H}ln\left(1-P_b^{\frac{1}{K_2}}\right)\Phi_2\right)^{\frac{1}{M_2}},\end{aligned} \tag{5.24}$$

where $\Phi_2 = \Phi\left(M_2\right) = \phi^{M_2}$.

The conversion gain

$$\begin{aligned} G_c &= \frac{\rho_2}{\rho_1} \\ &\approx \left(H^{\frac{1}{M_1}-\frac{1}{M_2}}\right) \\ &\cdot \left(\frac{-ln\left(1-P_b^{\frac{1}{K_2}}\right)}{1-\Phi_2-\frac{1}{H}ln\left(1-P_b^{\frac{1}{K_2}}\right)\Phi_2}\right)^{\frac{1}{M_2}} \\ &\cdot \left(\frac{-ln\left(1-P_b^{\frac{1}{K_1}}\right)}{1-\Phi_1-\frac{1}{H}ln\left(1-P_b^{\frac{1}{K_1}}\right)\Phi_1}\right)^{-\frac{1}{M_1}}. \end{aligned} \tag{5.25}$$

For $M_1K_1 = M_2K_2$, we multiplex the above equation with $\frac{P_b^{\frac{1}{K_1M_1}}}{P_b^{\frac{1}{K_2M_2}}}$, and the conversion gain can be represented as:

$$G_c \approx \left(H^{\frac{1}{M_1}-\frac{1}{M_2}}\right)(\beta_1)^{\frac{1}{M_1}}(\beta_2)^{-\frac{1}{M_2}}, \tag{5.26}$$

where

$$\beta_i = \frac{P_b^{\frac{1}{K_i}}\left(1-\Phi_i-\frac{1}{H}ln\left(1-P_b^{\frac{1}{K_i}}\right)\Phi_i\right)}{-ln\left(1-P_b^{\frac{1}{K_i}}\right)}, \quad for\ i=1,2. \tag{5.27}$$

For $i = 1, 2$, let $x_i = P_b^{\frac{1}{K_i}}$, $y_i = -ln\left(1-P_b^{\frac{1}{K_i}}\right) = \sum_{j=1}^{\infty}\frac{x_i^j}{j}$. Then,

$$\begin{aligned} \beta_i &= \frac{x_i\left(1-\Phi_i+\frac{1}{H}y_i\Phi_i\right)}{y_i} \\ &= \frac{x_i}{y_i}(1-\Phi_i)+\frac{1}{H}\Phi_i x_i \\ &\approx \frac{x_i}{y_i}(1-\Phi_i). \end{aligned} \tag{5.28}$$

The approximation works well for large H and $P_b^{\frac{1}{K_i}}$ not too close to one. For $P_b = 0.001$, $\Phi_i = 0.31$, $H = 10$, $K_1 = 50$, the error is only around 8%.

$\frac{x_i}{y_i}$ is smaller than 1 and monotonously decreasing with K_i. For $K_2 < K_1$ and $M_2 > M_1$, $\left(\frac{x_1}{y_1}\right)^{\frac{1}{M_1}} < \left(\frac{x_2}{y_2}\right)^{\frac{1}{M_2}}$. Therefore, the maximum conversion gain is given by

$$\begin{aligned} G_{c,max} &< \left(H^{\frac{1}{M_1}-\frac{1}{M_2}}\right)(1-\Phi_1)^{\frac{1}{M_1}}(1-\Phi_2)^{-\frac{1}{M_2}} \\ &< \left(H(1-\Phi_1)\right)^{\frac{1}{M_1}-\frac{1}{M_2}}, \end{aligned} \tag{5.29}$$

where $M_2 > M_1$.

Notation	Definition
D	Dimension set of the optical multiplexing of the network
d_i, d_j	A dimension of the optical multiplexing of the network
N_i	Total number of channels on dimension d_i
E	Convertible dimension set
$\bar{E}$	Non-convertible dimension set
N	Total number of channels per link
K	Number of trunks per trunk
M	Number of channels per trunk
F	Number of wavelengths per fiber
T	Number of slots per frame in TDM domain
k	the index of K
ρ	Uniform link load, or the busy probability of a channel
Δ	Switch size
H	Number of hops of a lightpath
$\bar{H}$	Average number of hops of the lightpaths in a network
ϕ	Link correlation
q_i	Busy probability of a trunk on the $i^{th} hop$
Φ	Trunk correlation
G_u	Utilization gain
n	Number of dimensions in a multi-dimensional network
m	Number of convertible dimensions
G_c	Conversion gain (improvement in network utilization)
S	Expanding factor

Table 5.1: Notations used in Chapter 5.

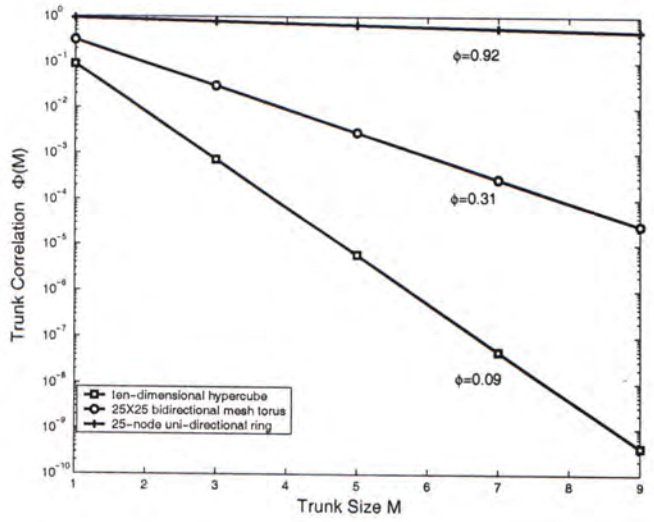

Figure 5.3: Traffic correlation versus the trunk size in a trunk switched network.

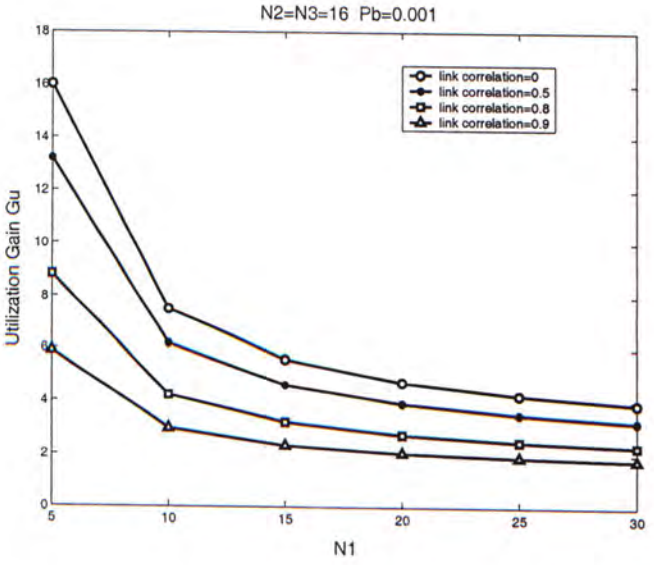

Figure 5.4: Utilization gain by multiplexing versus the original channel number for the networks with different link correlation.

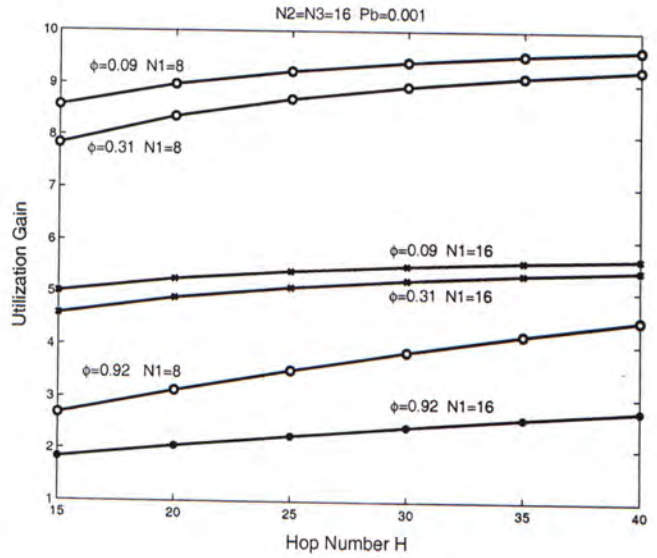

Figure 5.5: Utilization gain by multiplexing versus hop numbers for the networks with different original channel number N_1.

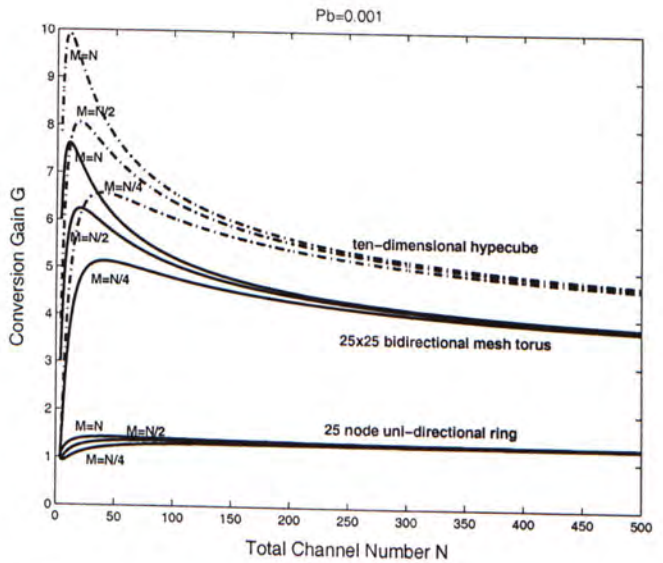

Figure 5.6: Conversion gain versus total number of channels.

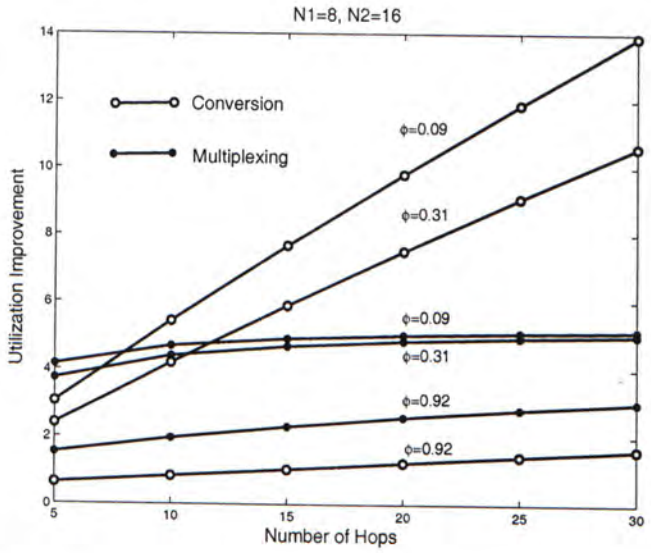

Figure 5.7: Utilization improvement (by multiplexing or by conversion) versus number of hops H.

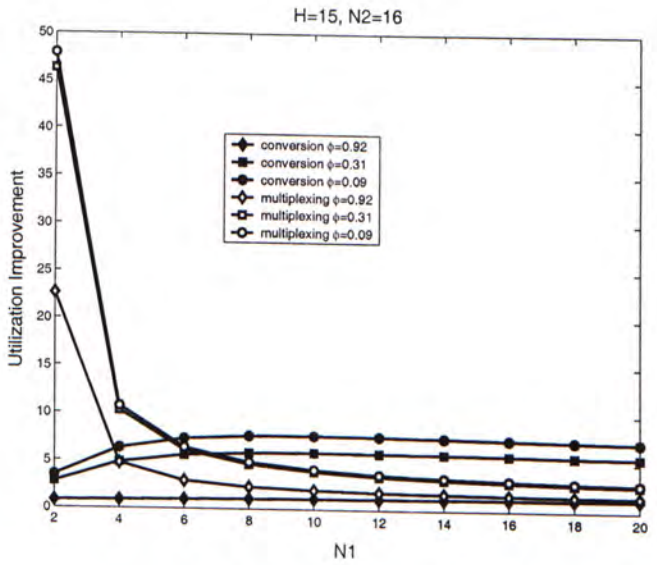

Figure 5.8: Utilization improvement (by multiplexing or by conversion) versus N1.

Chapter 6

Conclusion

6.1 Summary of the Thesis

In this thesis, the blocking performance of a code/wavelength routing network is presented. Two decomposition schemes are proposed to facilitate the investigation of the inclusive converted network. Also, by a generalized trunk switched model, the performance of the multi-dimensional optical routing networks are analyzed, including the blocking probability, network utilization and optical conversion gain.

Chapter 2 presents the enabling technologies for three types multi-dimensional optical routing networks, including the optical conversion technologies, optical transmitters, optical filters, etc. The schematic and the experimental setup are demonstrated.

Chapter 3 investigates the blocking performance arising from the limited conversion capability in a code/wavelength routing network. The numerical results show that the code conversion achieves higher conversion gain for the network with lower traffic load. When a small number of code converters are provided, the improvement of the blocking probability is the most significant.

Chapter 4 proposes an iterative decomposition scheme to facilitate the analysis on the blocking probability for a class of multi-dimensional routing networks. Extended trunk switched model is described.

In Chapter 5, an analytic model is proposed for studying the network utilization of generalized multi-dimensional optical routing networks. It is found that the utilization gain by adding new dimensions is closely related to the link correlation of the network. Less link correlated network will achieve more

significant utilization gain when new dimensions are added. It is also found that, the utilization gain is fairly insensitive to the network size. We derive, for the first time, closed-form solutions for the conversion gain in a partially or fully convertible n-dimensional optical routing network. From the comparison of the utilization gain by multiplexing (adding new dimensions) with the conversion gain, we find that highly correlated networks can obtain higher utilization gain by multiplexing than by conversion. Also, small networks and the networks with small number of channels benefit more from multiplexing than from conversion.

6.2 Future Work

For future work, it could be classified into two aspects, one is the experimental work, and the other is theoretical work.

The multi-dimensional switch is not mature currently, which will be one of the barriers for the implementation of the multi-dimensional optical routing networks. The three dimensional optical switch that can switch on the fiber, wavelength and time dimensions is promising for future application.

The network topology (in terms link correlation) is considered for the performance analysis on the homogeneous multi-dimensional optical networks. One of the future theoretical work could be the investigation on the heterogeneous networks. This would lead to the analysis on the optimal converter placement in a multi-dimensional networks with heterogeneous nodes.

Besides, the analysis on the blocking performance can be extended to the multi-dimensional networks with multicasting in optical layer.

In this thesis, binomial model is used for the investigation of the qualitative behavior of the multi-dimensional networks. Another possible future work is to take the traffic model into account and obtain accurate numerical results for the blocking probability under different traffic pattern.

Bibliography

[1] X. Yuan and A. Fulay, "Wavelength assignment to minimize the number ofsonet adms in WDM rings," in *Communications, 2002. ICC 2002. IEEE International Conference on*, vol. 5, pp. 2917 –2921, 2002.

[2] D. Zhemin and M. Hamdi, "A simple routing and wavelength assignment algorithm using the blocking island technique for all-optical networks," in *Communications, 2002. ICC 2002. IEEE International Conference on*, vol. 5, pp. 2907 –2911, 2002.

[3] P. Manohar, D. Manjunath, and R. Shevgaonkar, "Routing and wavelength assignment in optical networks from edge disjoint path algorithms," *IEEE Communications Letters*, vol. 6, pp. 211 –213, May 2002.

[4] A. Narula-Tam, P. Lin, and E. Modiano, "Efficient routing and wavelength assignment for reconfigurable WDM networks," *Selected Areas in Communications, IEEE Journal on*, vol. 20, pp. 75 –88.

[5] R. Sendag, P. fei Chuang, and D. Du, "Routing and wavelength assignment in optical passive star networks with non-uniform traffic load," *Global Telecommunications Conference, 2001. GLOBECOM '01. IEEE*, vol. 3, pp. 1435–1439, 2001.

[6] R. A. Barry and P. A. Humblet, "Models of blocking probability in all-optical networks with and without wavelength changers," *IEEE Journal on Selected Areas in Communications*, vol. 14, pp. 858–867, June 1996.

[7] M. Kovacevic and A.Acampora, "On wavelength translation in all-optical networks," in *Proceedings of IEEE INFOCOM*, vol. 2, pp. 413–422, Apil 1995.

[8] G. Maier, M. Martinelli, A. Pattavina, and M. Scappini, "Performance of WDM rings with wavelength conversion under non-poisson traffic," in *Proceedings of IEEE ICC*, vol. 3, pp. 2037 –2041, 1999.

[9] G. Shen, S. K. Bose, T. H. Cheng, C. Lu, and T. Y. Chai, "Operation of WDM networks with different wavelength conversion capabilities," *IEEE COMMUNICATIONS LETTERS*, vol. 4, pp. 239–241, Jul. 2000.

[10] S. Subramaniam, M. Azizoglu, and A. K. Somani, "On optimal converter placement in wavelength-routed networks," *IEEE/ACM Transaction on Networking*, vol. 7, pp. 754–766, Oct. 1999.

[11] S. Subramaniam, M. Azizoglu, and A.K.Somani, "Allcoptical networks with spare wavelength conversion," *IEEE/ACM Transaction on Networking*, vol. 4, pp. 544–557, Aug. 1996.

[12] A. Birman, "Computing approximate blocking probabilities for a class of all-optical networks," *IEEE Journal on Selected Areas in Communications*, vol. 14, pp. 852 –857, June 1996.

[13] E. Karasan and E. Ayanoglu, "Effects of wavelength routing and selection algorithms on wavelength conversion gain in WDM optical networks," *IEEE GLOBECOM*, Nov 1996.

[14] S. Subramaniam and R. Barry, "Wavelength assignment in fix routing WDM networks," *IEEE ICC*, Nov. 1997.

[15] T. Lee, K. Lee, and S. Park, "Optimal routing and wavelength assignment in WDM ring networks," *IEEE Journal on Selected Areas in Communications*, vol. 18, pp. 2146–2154, Oct. 2000.

[16] M. Mellia, E. Leonardi, M. Feletig, R. Gaudino, and F. Neri, "Exploiting OTDM techology in WDM networks," *IEEE INFOCOM*, 2002.

[17] J. Sharony, T. E. Stern, and Y. Li, "The universality of multidimensional switching networks," *IEEE Transactions on Networking*, vol. 2, pp. 602–612, Dec. 1994.

[18] J. Pfeiffer, T.and Kissing, J.-P. Elbers, B. Deppisch, M. Witte, H. Schmuck, and E. Voges, "Coarse WDM/CDM/TDM concept for optical packet transmission in metropolitan and access networks supporting 400 channels at 2.5 gb/s peak rate," *Journal of Lightwave Technology*, vol. 18, pp. 1928–1938, Dec. 2000.

[19] J. Yates, J. Lacey, and D. Everitt, "Blocking in multiwavelength TDM networks," *Telecommunications Systems Journal*, vol. 12, pp. 1–19, 1999.

[20] R. Srinivasan and A. K. Somani, "A generalized framework for analyzing time-space switched optical networks," *IEEE Journal on Selected Areas in Communications*, vol. 20, pp. 202–215, Jan. 2002.

[21] G. Keiser, *Optical Fiber Communications.* McGraw-Hill higher education, 2000.

[22] C. kit Chan, "Optical packet switching," *seminar*, 2000.

[23] X. Hou and H. Mouftah, "Towards optimal design of wavelength-convertible optical switches for the all-optical next-generation internet," in *Electrical and Computer Engineering, 2001. Canadian Conference on*, vol. 1, pp. 441 –446, 2001.

[24] E. Ciaramella, "Introducing wavelength granularity to reduce the complexity of optical cross connects," *IEEE Photonics Technology Letters*, vol. 12, pp. 699–701, June 2000.

[25] M. Nishimura, K.and Tsurusawa and M. Usami, "Wavelength conversion with no pattern effect at 40 gbps using an electroabsorption waveguide as a phase modulator," *Optical Fiber Communication Conference and Exhibit, 2001*, vol. 3, pp. WK5 –1–3.

[26] S. Nakamura, Y. Ueno, and K. Tajima, "168-gb/s all-optical wavelength conversion with a symmetric-mach-zehnder-type switch," *IEEE Photonics Technology Letters*, vol. 13, pp. 1091 –1093, Oct. 2001.

[27] V. Perlin and H. Winful, "All-fiber wavelength conversion using cross-phase modulation and bragg gratings," *IEEE Photonics Technology Letters*, vol. 14, pp. 176 –178, Feb. 2002.

[28] B. Sarker, T. Yoshino, and S. Majumder, "All-optical wavelength conversion based on cross-phase modulation (xpm) in a single-mode fiber and a mach-zehnder interferometer," *IEEE Photonics Technology Letters*, vol. 14, pp. 340 –342, Mar. 2002.

[29] M. Westlund, J. Hansryd, P.A.Andrekson, and S.N.Knudsen, "Transparent wavelength conversion in fibre with 24 nm pump tuning range," *Electronics Letters*, vol. 38, Jan. 2002.

[30] C. Joergensen, S. Danielsen, and K. Stubkjaer, "All-optical wavelength conversion at bit rates above 10 Gb/s using semiconductor optical amplifiers," *Selected Topics in Quantum Electronics, IEEE Journal on*, vol. 3, pp. 1168–1180, Oct. 1997.

[31] B. Ramamurthy, *Design of optical WDM networks: LAN, MAN and WAN architectures.* Boston : Kluwer Academic PublisherS, 2001.

[32] N.Wada and K. Kitayama, "10gb/s optical code division multiplexing using 8-chip optical bipolar code and coherent detection," *JLT*, vol. 17, pp. 1758–1765.

[33] K. ichi Kitayama, "Code division multiplexing lightwave networks based upon optical code conversion," *IEEE Journal on Selected Areas in Communications*, vol. 16, pp. 1309 –1319, Sep. 1998.

[34] I. Andonovic, H. Sotobayashi, N. Wada, and K.-I. Kitayama, "Experimental demonstration of the (De)Coding of hybrid phase and frequency codes using a pseudolocal oscillator for optical code division multiplexing," *IEEE Photonics Technology Letters*, vol. 10, pp. 887–889, June 1998.

[35] W. Huang and I. Andonovic, "Coherent optical pulse CDMA systems based on coherent correlation detection," *IEEE TRANSACTIONS ON COMMUNICATIONS*, vol. 47, no. 2, pp. 261–271, 1999.

[36] H. Sotobayashi, W. Chujo, and K. Kitayama, "1.52 tbit/s OCDM/WDM (4 ocdm/spl times/19 WDM/spl times/20 gbit/s) transmission experiment," *Electronics Letters*, vol. 37, pp. 700 –701, May. 2001.

[37] Y. G. Wen, L.K.Chen, and F. Tong, "Fundamental limitation and optimization on optical code conversion for WDM packet switching networks," in *Proceedings of OFC*, pp. TUv–5, Mar. 2001.

[38] X. Zhang, Y. Ji, and X. Chen, "Code routing technique in optical network," *Communications, 1999. APCC/OECC '99. Fifth Asia-Pacific Conference on ... and Fourth Optoelectronics and Communications Conference*, vol. 1, pp. 416 –419, 1999.

[39] K. Kitayama, N. Wada, and H. Sotobayashi, "Architectural considerations for photonic ip router based upon optical code correlation," *Journal of Lightwave Technology*, vol. 18, pp. 1834 –1844, Dec. 2000.

[40] Y.G.Wen, Y.Zhang, and L.K.Chen, "On architecture and limitation of optical multiprotocol label switching (MPLS) networks using optical-orthogonal-code (OOC)/wavelength label," *Optical Fiber Technology*, vol. 8, 2002.

[41] Y.G.Wen, Y.Zhang, L.K.Chen, and F. Tong, "On scalability of an optical routing network based on code/wavelength label switching," *Submitted to IEEE Photonics Technology Letters*, 2002.

[42] K.Kitayama, "Error-free 1.24 gb/s 4-chip coherent CDM code converter," *ECOC*, 1997.

[43] P. Petropoulos, N. Wada, P. Teh, and W. K. K.-I. Ibsen, M.and Chujo, "Demonstration of a 64-chip ocdma system using superstructured fiber gratings and time-gating detection," *IEEE Photonics Technology Letters*, vol. 13, pp. 1239 –1241, Nov. 2001.

[44] H. Geiger, A. Fu, P. Petropoulos, M. Ibsen, D. Richardson, and R. Laming, "A 8x8 all optical space-switch based on a novel 8x1 moems switching module," in *Optical Communication, 1998. 24th European Conference on*, vol. 1, pp. 337–338, 1998.

[45] P. C. Teh, P. Petropoulos, M. Ibsen, and D. Richardson, "A comparative study of the performance of seven- and 63-chip optical code-division multiple-access encoders and decoders based on superstructured fiber bragg gratings," *Journal of Lightwave Technology*, vol. 19, pp. 1352 – 1365, Sep. 2001.

[46] D. Sampson, N. Wada, K.Kitayama, and W. Chujo, "Demonstration of reconfigurable all-optical code conversion for photonic code-division multiplexing and networking," *Electronics Letters*, vol. 36, pp. 445–447, Mar. 2000.

[47] K. Sotobayashi, H.and Kitayama, "All-optical code conversion of 10 gb/s bpsk codes without wavelength-shift by cross-phase modulation for optical code division multiplexing networks," in *Proceedings of Optical Fiber Communication Conference, 2000*, vol. 2, pp. 163–165, 2000.

[48] J.W.Kang, J.S.Kim, C.M.Lee, E.Kim, and J.J.Kim, "1x2 all-optical switch using photonchromic-doped waveguides," *Electronics Letters*, vol. 36, pp. 1641–1643, Sep. 2000.

[49] C.Kim, D.A.May-Arrioja, and J.Pamulapati, "Ultrafast all-optical multiple quantum well integrated optic switch," *Electronics Letters*, vol. 36, pp. 1929–1930, Nov. 2000.

[50] C. Matos, M.Pugnet, and A. Corre, "Ultrafast coherent all-optical switching in quantum-well semiconductor microcavity," *Electronics Letters*, vol. 36, pp. 93–94, Jan. 2000.

[51] D. Hunter and D. Smith, "New architectures for optical TDM switching," *Journal of Lightwave Technology*, vol. 11, pp. 495–511, Mar. 1993.

[52] J. Yao, P. Barnsley, N. Walker, and M. O'Mahony, "An experimental photonic time slot interchanger using semiconductor laser amplifiers and fibre delay lines," *Optical Switching, IEE Colloquium on*, pp. Page(s): 7/1 –7/5, 1993.

[53] H.F.Jordan, D.Lee, K.Y.Lee, and S.V.Ramanan, "Serial array time slot interchangers and optical implementations," *IEEE Transactions on Computers*, vol. 43, pp. 1309–1318, Nov. 1994.

[54] Y. G. Wen, L.K.Chen, K. P. Ho, and F. Tong, "All-optical code converter scheme for OCDM routing network," in *Proceedings of ECOC*, pp. 1088–1090, Sep. 2000.

[55] S. Taccheo, "Amplitude noise and timing jitter of pulses generated by supercontinuum spectrum-slicing for data-regeneration and tdm/wdm applications," in *Proceedings of Optical Fiber Communication Conference, 2001*, vol. 3, pp. WP2 –1–3, 2001.

[56] G. Jeong and E. Ayanoglu, "Comparison of wavelength-interchanging and wavelength-selective cross-connects in multiwavelength all-optical networks," *IEEE INFOCOM*, vol. 1, pp. 156–163, 1996.